AMES / GRANT / IN-74

71793-CR

479

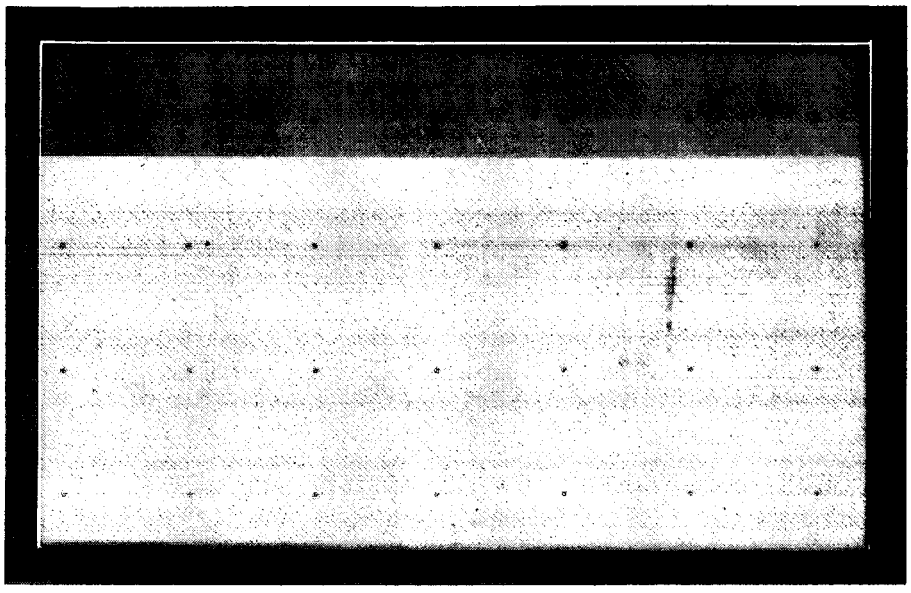

(NASA-CR-180604) INFRARED FIBER OPTIC MATERIALS Final Technical Report, 1 Jan. 1983 - 31 Dec. 1985 (Stanford Univ.) 47 p Avail: NTIS HC A03/MF A01 CSCL 20F

N87-23257

Unclas

G3/74 0071793

CENTER FOR MATERIALS RESEARCH

STANFORD UNIVERSITY • STANFORD, CALIFORNIA

The Board of Trustees of the
Leland Stanford Junior University
Center for Materials Research
Stanford, CA 94305
Santa Clara, 12th Congressional District

Final Technical Report

on

Infrared Fiber Optic Materials

for the period

01/01/83 through 12/31/85

Contract Number NCC-2-22

CMR-87-3

Submitted to
National Aeronautics and Space Administration
Ames Research Center
Moffett Field, California 94305

Principal Investigator

Robert S. Feigelson
Professor (Research)
Center for Materials Research
Crystal Science and Engineering

May 21, 1987

TABLE OF CONTENTS

I. INTRODUCTION

This report summarizes a 36-month cooperative research program between NASA/Ames and the Center for Materials Research at Stanford University on the development of IR fiber optics for use in astronomical and other space applications. The program sought to identify candidate materials for use in the 1-200 μm and the 200-1000 μm wavelength range; to carry out synthesis and optical characterization of several of these materials in bulk form; and to study the fabrication of a few materials in single crystal fiber optic form.

Funding levels for the program were:

Period	01-01-83 to 06-30-84	$42,569
	07-01-84 to 12-31-85	30,000
	Net Total Support	$72,569

One graduate student was partially supported during the first year of the program. Thereafter, staff personnel were used for the research activities.

II. BACKGROUND

The need for wide bandwith communications has been the main driving force for the development of fiber optics. While there are a few examples of polymer-based fibers operating in the visible portion of the spectrum, such as the polymethyl methacrylate cables by Du Pont, fused silica-based glassy fibers operating at 1 μm currently dominate the optical communications field. The optical absorption of fused silica, however, rises rapidly at wavelengths in excess of 1.5 μm, and this limits the utility of silica-based fibers to wavelengths shorter than 4-5 μm. It becomes evident upon inspection that there are only a few good glassformers which transmit much beyond 8 μm. Examples from this group currently under study are the HfF_4-based glasses with minimum dispersion slightly under 2 μm, the ZrF_4-ThF_4-BaF_2 glasses which transmit to 8 μm (1), and As_2Se_3 glass which transmits to 12 μm (2).

There are a large number of crystalline compounds, however, which do transmit far into the IR, some in excess of 50 μm. These include mostly the binary and ternary halides, and a few selected oxides and chalcogenides. It is certainly the case that much less work has been carried out to study IR transmitting materials in single crystal fiber form compared to fused silica fibers. Some work has been carried out on As_2S_3 and As_2Se_3 glasses in fiber form (2). A number of halides, such as AgCl and AgBr (3), and KRS-5 and Tl-Br (2), have been extruded as polycrystalline fibers. However, the heavy metal halides have relatively high indices of refraction and are less desirable than low index materials. In addition, polycrystalline fibers have the usual problems associated with grain boundaries. Impressive results have recently been reported in the domestic and Japanese literature on the growth of single crystal optical fibers of low melting halides, such as AgBr (4) and KRS-5 (5). Uniform, IR transparent single crystal fibers have been grown in lengths exceeding one meter.

While these advances are fairly impressive, the difficulties in fabricating single crystal materials in fiber optic form are sufficiently great that it is safe to assume they will never be suitable as passive transmission media at lengths over a few meters. In fact, the greatest application for single crystal optical fibers will likely be in lengths of only a few millimeters to a few centimeters - in applications which make use of their unique properties such as optical anisotropy, electro-optic activity and optical nonlinearity.

At the time this cooperative effort was conceived, the single crystal fiber growth program at Stanford was being rapidly expanded to include the preparation of a wide range of materials by using both an existing laser-heated pedestal growth technique and a variation of a process used by Bridges (4) which we refer to as the capillary-fed fiber growth technique. It was natural therefore that an exploratory program on IR transmitting optical fiber materials be carried out here.

III. APPROACH

During the first year of this program two areas of emphasis were selected. The main effort was directed to the preparation of single crystal optical fibers of the chalcopyrite compound $AgGaS_2$ for heterodyne detection of mid infrared wavelenths using silicon-based detector technology. $AgGaS_2$ at the time was under active study in this laboratory for nonlinear applications in bulk crystal form. Crystals were being grown by the vertical Bridgman method and characterized by conventional optical methods. It was decided to apply several optical fiber growth techniques to this material to determine if it could be fabricated as a single crystal optical fiber with high enough optical quality to be of practical use.

A much smaller effort was simultaneously devoted to the preparation of KRS-5 in single crystal fiber form using equipment and techniques developed previously at Stanford with support from the Naval Research Laboratories.

IV. TECHNICAL SUMMARY

A. Growth of $AgGaS_2$ in Optical Fiber Form

This material and its closely-related cousin, $AgGaSe_2$, are currently the best understood of the chalcopyrite compounds that are known to be highly useful as mixers and doublers in the IR. $AgGaS_2$ has shown to be continuously phase-matchable throughout its entire transparency region from 0.45-12 μm. Lacking strong temperature tuning characteristics to achieve specific phase matching conditions, $AgGaS_2$ rods must be cut (or grown) within narrow orientational limits. The development of techniques to grow clear, oriented $AgGaS_2$ rods along particular crystallographic directions therefore contituted the main research challenge. The specific wavelenths being sought for frequency shifting to the 1 μm region by difference frequency generation, and the required phase matching angles assuming a 1.06 μm Nd:YAG pump wavelenth were:

Signal	Pump	Phasematching Angle
12.4 μm	1.064 μm	40° Type II
8 μm	1.064 μm	50° Type II
4 μm	1.064 μm	90° Type II

In the bulk crystal growth of this material, which is normally carried out in sealed fused silica ampoules at 996°C, it is possible to grow crystals only along or near to the c-axis. This is due to the anomolous thermal properties of $AgGaS_2$ which cause it to expand along the c-axis during cooling. If the c-axis is tipped too far from the axis of the growth ampoule, a net transverse expansion can occur during cooling which produces a disasterous result both on the crystal and on the fused silica ampoule. The desire to grow $AgGaS_2$ fibers with the c-axis tipped 40°-90° off the fiber axis thus posed some concern.

All of the crystal growth experiments carried out on the preparation of single crystal fibers were based on our long experience with the growth of bulk $AgGaS_2$ crystals. A complete technical report of the highly successful results from that work are included in this document as Appendix I. In fact, a portion of the funding for this program was devoted to studies of optical defects in bulk crystals which is covered rather thoroughly in the appended document.

Because of the anticipated difficulties in growing $AgGaS_2$ in single crystal fiber form, a number of different approaches were undertaken. These are summarized in Table 1 and each is discussed in turn in the following sections.

1. Direct Fusion by the Laser-Heated Pedestal Growth Method

The first set of experiments was carried out in the laser-heated pedestal growth (LHPG) apparatus which is described in Appendix II. This method is ideally suited to the growth of materials where one must be concerned about mechanical constraint since none occurs. The cross-section of the growing fiber crystal is controlled essentially by surface tension effects and growth rate anisotropy.

TABLE 1

$AgGaS_2$ Growth Method	Growth Temperature	Equipment
Direct growth from the melt (open system)	996°C	Laser Heated Pedestal Growth Apparatus
Direct growth from the melt (encapsulated, warm wall, capillary system)	996°C	Miniature zone refiner
Solution growth from Sb_2S_3 (encapsulated, hot wall, capillary system)	550-600°C	Modified miniature zone refiner

$AgGaS_2$ melts congruently at 996°C and is known to be somewhat volatile at its melting point. In the LHPG growth method, however, growth rates of typical fibers can approach millimeters/minute and total time at temperature for each section of fiber can be only a few seconds. It was therefore decided that this method should be the first to be evaluated.

Experimental Procedures

Feedstock from bulk grown crystals was prepared in the form of 1 mm^2 bars approximately 3 cm long in the c-direction. The choice of orientation was dictated by the need for a c-axis seed which is the only growth direction suitable for Bridgman type growth due to the expansion problems discussed earlier. A flowing argon ambient was used in the growth chamber during the melting experiments because reactivity seems to be greater in oxygen-containing environments.

Results

In all attempts to achieve a molten zone using both slow and fast heating rates, significant evaporation was observed at temperatures below the melting point. At the melting point evaporation was so rapid that steady-state growth was impossible. Upon cooling, the solidified melt was found to be black and metallic in appearance, fig. 1, indicating chemical decomposition had occurred.

Discussion

Although the LHPG system does cause a degree of superheating due to the tightly focused laser beam, it was concluded that $AgGaS_2$ is simply too reactive and volatile near its melting point to be grown in an open system. Even though the vapor pressure of sulfur over $AgGaS_2$ is low, thought to be only a few tens of microns at the melting point, this is evidently sufficient to allow decomposition to occur in an open system particularly when the surface area to volume ratio is very large as it is in fiber growth. The results of these experiments suggested that we would either have to accomplish a significant reduction in growth temperature in order to continue using an open system, or resort to a sealed quartz system.

2. Capillary Growth Directly from the Melt

The second approach investigated involved the melt growth of $AgGaS_2$ inside a 1 mm ID fused quartz capillary tube. The basic arrangement is shown in fig. 2a. Growth in this "floating zone" procedure is carried out by creating a small molten zone with a localized heater, and then causing the molten zone to pass along the feed rod by translating the heater.

Experimental Procedures

For these experiments, several 1 mm diameter rods of $AgGaS_2$ previously grown by the vertical Bridgman method were fabricated. The orientation was chosen with the axis of the rods along the c-axis, which was done to eliminate any thermal expansion problems at first. Prior to loading, the fused quartz capillaries were coated with a thin layer of carbon through which light could pass by the pyrolysis of acetone vapor. (A thin coating of pyrolytic carbon is known to be essential in order to prevent reaction between $AgGaS_2$ at its melting point and the fused quartz capsule.) After loading several of the $AgGaS_2$ rods, the capillaries were evacuated, then back-filled with purified argon (0.5 atm) and finally sealed off. The argon backfill was used to minimize the transport of sulfur within the growth capillary due to thermal gradients present during growth.

The basic thermal geometry used for these experiments was a "broad" peak as shown in fig. 2b. The furnace itself was constructed of three closely spaced turns of supported Kanthal wire and this was surrounded by a gold-coated quartz reflector as shown in fig. 3. Provisions were made to view the capillary tube in the region of the hot zone: with the thin transparent coating of pyrolytic carbon on the interior of the capillary it was hoped we would be able to see the molten zone.

The furnace system used was a commercial zone refiner originally designed for low melting organic compounds and rebuilt for these experiments.

Experiments were carried out first with the growth zone stationary to observe molten zone behavior and then with the molten zone translating uniformly upward at a rate of 1 mm/hour which is close to the rate used for bulk growth of $AgGaS_2$ crystals in 27 mm diameter sizes. After several hours of growth, the capillaries were cooled slowly and sectioned for microscopic examination.

Results

With T_{max}=1040°C a molten zone of ~ 2 mm in height was established. Immediately upon melting, many surface bubbles were observed in the molten zone. The bubbles were active, continued to form for 10 minutes and then became more quiescent. Uniform growth was then carried out. Several of the capillaries were found to be cracked after cooling, fig. 4a. After mounting and sectioning it was observed that serious decomposition of the $AgGaS_2$ had occurred in the molten zone. Residual material was black, indicating sulfur deficiency, fig 4b. Furthermore, voids were found which indicate that the liquid bridge between the source and seed segments of the charge had broken when the exsolution of a gas phase had occurred during solidification as shown in fig. 4b. Further inspection of the samples indicated that where the $AgGaS_2$ melted, there was a strong mechanical interaction with the fused quartz capillary leading to the extensive cracking of the crystal as shown in fig. 4c.

Discussion

The growth of $AgGaS_2$ directly from the melt in fused quartz capillaries, on the basis of these experiments, does not seem promising. The primary problems, surface bubble formation on the capillary walls and interaction with the fused quartz capillaries, are difficult to overcome. (Surface bubble formation occurs in bulk growth of $AgGaS_2$ as well, and in bulk growth only the use of precision tapered fused quartz growth ampoules and accurate c-axis seeding make possible the successful extraction of the boules from their fused quartz growth ampoule.)

A more promising approach was felt to be the lowering of the growth temperature by solution growth methods.

3. Growth from Solution by the Travelling Heater Method

The first problem encountered in solution growth is identifying an optimum solvent. Ag_2S, itself a constituent of $AgGaS_2$, is one possibilty and it has been used with some, but not total, success in this laboratory for the preparation of bulk crystals. These experiments are described in Appendix I. A potential advantage of low temperature flux is that precipitate-free $AgGaS_2$ might be obtained. Using Ag_2S as a solvent, we did show that it is possible to grow $AgGaS_2$ free of precipitates by choosing a composition to yield a liquidus temperature at or below 900°C. Ag_2S cannot be used at temperatures much below 800°C, however, and in this temperature range, surface bubbles at the walls and interaction with fused quartz ampoules still occur. For that reason we did not consider it a practical flux for these studies.

Two relatively low temperature fluxes for $AgGaS_2$ have been developed at the Hughes Research Laboratories by Sashital (6, 7) for LPE growth of low resistivity $AgGaS_2$ layers. The two fluxes are Sb_2S_3, which forms a eutectic with $AgGaS_2$ at 495°C, and KCl, which forms a eutectic with $AgGaS_2$ at 732°C. The phase equilibria are shown in Figure 5. Although KCl is more attractive from the point of view of being easily removed with water, operating temperatures are in the 800°C range. With Sb_2S_3 significantly lower temperatures in the 600°C range are possible. Furthermore, from the LPE results of Sashital, better layer morphology appeared to result from the Sb_2S_3 flux. Hence Sb_2S_3 was chosen for evaluation by the travelling solvent method.

The optical quality of $AgGaS_2$ grown from Sb_2S_3 solutions is not well established from the previously referenced work (6) since path lengths for their optical propagation requirements were very short. Optical path lengths in our projected applications were anticipated to be in the order of 1 cm and hence optical quality was important to determine and control.

Experimental Procedures

One of the conclusions from our melt growth experiments just described was that $AgGaS_2$ requires a hot wall environment to prevent decomposition of the molten material. The furnace assembly in the zone refiner was therefore rebuilt as a 550°C "C"-shaped heat pipe with a 600°C spike in the center, fig. 6. The objective of this design was to maintain the entire charge at 550°C except for the narrow molten zone maintained somewhat hotter (600°C) by the spike heater. In order to enhance melt interface stability it is desirable to create a relatively short molten zone with high thermal gradients at the dissolving and recrystallizing interfaces. Hence the thermal spike was made as short as possible. A typical temperature gradient is shown in fig. 7. Similar 1 mm ID fused quartz capillaries were used and the same c-axis 1 mm diameter $AgGaS_2$ feedstock was used as well. The important difference however was the addition of a 50 mg pellet of Sb_2S_3 also shown in fig. 7. It was estimated that at 600°C this amount of Sb_2S_3 in contact with solid $AgGaS_2$ should have yielded a molten zone of $\sim$ 2 mm in length. As in the melt growth experiments a transparent coating of pyrolytic carbon was applied to the interiors of the capillaries and an 0.5 atm backfill of purified argon was used prior to sealing off.

The zone refiner gearbox was rebuilt to achieve the slow translation rates that are required for solution or flux growth. While crystals can be grown from pure melts at growth rates of approximately 1 mm/hour, stable growth from solvents rarely exceeds 1 mm/day. Growth rates used in our experiments were 0.5 mm/day and experiments varied in length up to 20 days. At the termination of growth, the furnaces were cooled at $\sim$ 200°C/min.

Results

Quartz capillaries could be inspected at temperature in the heat pipe furnce through a viewing aperature. When the spike temperature

reached approximately 600°C, wetting of the quartz walls by molten solvent could be seen. However, it was not possible to determine if surface bubbles were present or if the liquid zone spanned the gap between the source and feed rods. (The zone was moved upwards and since the feed rod was unsupported in the quartz capillary, gravitational settling was assumed to consolidate the molten zone.

Quartz capillaries survived the growth and cooling uncracked as opposed to the melt growth situation where cracking occurred. When the growth ampoules were sectioned it could clearly be seen that melting of the Sb_2S_3 solvent had occurred and that the $AgGaS_2$ in contact with the molten solvent had not decomposed to any appreciable extent. Unfortunately it was also found that the molten zone had developed voids and/or broken down into several segments, Figure 8. A clean transverse liquid-solid interface was not found. Nor was any strong evidence of molten zone movement seen. No recrystallized $AgGaS_2$ was found under microscopic examination from which evaluation of optical quality could have been made.

Discussion

The main conclusions drawn from these solution growth experiments were that surface tension effects in 1 mm size capillaries are sufficient to cause breakup of Sb_2S_3 solvent zones in contact with $AgGaS_2$, and slow volatilization of a vapor species probably still occurs leading to the formation of voids in the capillary. Reactivity with the carbonized quartz capillaries did not appear to be a problem.

4. Fabrication of $AgGaS_2$ Rods from Bulk Crystals

While the crystal growth experiments were in progress, several 1 mm diameter rods of nominally 1 cm in length were fabricated from bulk material. The purpose in doing this was to test their handling properties, end face polishing difficulties, and tuning problems due to geometrical aperturing with tuning angle. With $AgGaS_2$ crystals, the exact phase matching conditions must be achieved by angle tuning: the temperature tuning coefficients are too small for effective use.

With long rods of small diameter, only small tuning angles are possible so their orientations become critically important. The axes of the rods must be within fractions of a degree of the phase matching angle. This constraint must apply both in growing long rods and in cutting them from bulk specimens. Oriented rods were prepared in two orientations, Type II, 41° and 50° which corresponds to phase matching for 12 μm and 8 μm, respectively, for up-conversion with a 1.06 μm pump wavelength. Bulk crystals were first cut and end faces polished normal to the propagation direction. Long square cross-section bars were then cut and these were carefully rounded on a precision micro centerless grinder so as to minimize chipping of the already polished end faces.

In general it was found that the 41° rods were more fragile than the 50° rods probably because the plane with easy cleavage, (112), is oriented in a more normal direction. This would not be a problem with rods having a highly polished surface because the surface defects where cleavage nucleates would be minimized.

In handling a wide variety of oxide fibers over the past six years we have found that the best way to polish end faces on a submillimeter rod is to first epoxy the rod into a glass or quartz capillary tube which then supports it during cutting and polishing. The prepolishing procedure was used for expediency.

The oriented and polished rods were delivered to NASA/Ames during the first 18 months of the program for testing and evaluation.

B. Growth of KRS-5 in Optical Fiber Form

The KRS-5 fiber growth technology was developed at Stanford under a program sponsored by NRL/DARPA. The basic configuration is based on a design developed by T. J. Bridges *et al.* (8). A schematic is shown in fig. 9. The main components of the system include: (1) a pressurized quartz reservoir and capillary feed tube, (2) a furnace with a separately adjustable afterheater, (3) a cold finger, (4) a fiber guiding x-y stage, (5) a fiber winding drum, (6) a quartz shroud over

the growth zone, (7) a pressurization system to pressurize the reservoir and capillary, and (8) precision temperature controllers for the furnace and after-heater. In this system configuration, the fibers are pulled upward during growth. They must also be totally constrained by the mechanical fiber guides because halide melts have very low viscosity.

The only serious problem encountered was fiber guiding above the growth interface. As Bridges did in his original work (8), we relied on a somewhat oversized and slightly curved teflon sleeve to guide the fiber as it is pulled from the melt and wound on the drum. The theory is that the fiber should touch the sleeve in only three places and that the fiber should be mechanically contrained. However, this technique has not proven to be very satisfactory because when slight diameter fluctuations come into contact with the teflon sleeve, the free end of the fiber in the melt moves sideways and this introduces a new diameter perturbation. We originally tried a number of modifications to the teflon sleeve geometry. However, none proved totally successful at eliminating perturbations and diameter fluctuations. During this program, several submillimeter KRS-5 fibers in the order of 10-20 cm long were prepared and delivered to NASA/Ames for evaluation. Their optical quality appeared to be very good in the short range, fig. 10. Diameter fluctuations of $\simeq$ 10% were present in these fibers, however, due to mechanical problems associated with guiding through the pulling apparatus. Core defects were occasionally observed in the narrow sections, probably due to inclusions caused by rapid growth rate fluctuations, fig. 11.

Major refinements in the mechanical pulling system used for the KRS-5 growth system to eliminate mechanical fluctuations during pulling were not made, but it was thought that the guiding problems could be solved through such modifications. The development of extruded polycrystalline fibers with reasonably low absorption coefficients, at the Hughes Research Laboratories and elsewhere, has allowed the evaluation of this material in short distance, long wavelength applications

C. Interdiffusion Studies in the $AgGaS_2$-$AgGaSe_2$ System

In the ensuing years since the beginning of this program, we have been seeking ways to increase the nonlinear optical converion efficiencies of a number of nonlinear optical materials. It was shown not long ago by Professor R. L. Byer at Stanford, that optical light guiding can greatly increase the high field interaction length in thin films and fibers over the conventional Rayleigh limited focused beam optics in bulk crystals. Hence much higher conversion efficiencies can be expected from light guiding in nonlinear media.

Given the original goals of this program which are in part achieving high conversion efficiences, it seemed appropriate to invest the final few months' efforts toward the creation of optical waveguiding in $AgGaS_2$. The approach was to look at the $AgGaS_2$-$AgGaSe_2$ pseudobinary system in which a complete series of solid solutions has been shown to exist (9). See fig. 12 for the pseudobinary phase equilibria in the system.

$AgGaSe_2$ is an isomorph of $AgGaS_2$, and has similar optical properties except that its index of refraction is slightly higher, 2.6 vs. 2.4 and its transparency range is at slightly longer wavelengths, 0.7 - 18 μm vs. 0.45 - 11 μm. Its nonlinear coefficients are somewhat higher than these of $AgGeS_2$ as well. Both crystals can be grown to approximately the same level of optical quality. Pure $AgGaSe_2$ cannot be phase matched for any wavelengths below 2.1 μm, however, and for that reason would not be a candidate for this program where pumping with 1.06 μm is desired. However, solid solutions of $(AgGaS_2)_{1-x}$-$(AgGaSe_2)_x$ where x is not too large would be expected to phase match. Such a composition would also be expected to have a somewhat higher index of refraction than pure $AgGaS_2$ and consequently should form a thin film optical waveguide. A long range goal would therefore be the fabrication of a thin film waveguiding structure like that shown in fig. 13 where a thin layer of mixed composition has been formed on a pure $AgGaS_2$ substrate. Such a structure could be deposited by the LPE technology of Sashital (6) or by diffusion. The

approach taken here was to undertake the study of diffusion between $AgGaS_2$ and $AgGaSe_2$, beginning with reactions occurring only through the vapor phase. Vapor phase interaction would hopefully limit surface damage to very thin layers or prevent it completely.

To complete a study such as this would require a substantial amount of graduate support and several years duration, far in excess of the limited resources and the brief amount of time invested here. However, this program has allowed us to get started. (Subsequent to its termination, follow-on funding to support phase equilibrium and related studies in $AgGaS_2$ and $AgGaSe_2$ was received from the Office of Naval Research. This work will therefore continue under their auspices.)

Experimental Procedures

The first objective was simply to find a set of experimental conditions where a vapor phase diffusion couple could be established between $AgGaS_2$ and $AgGaSe_2$. Random 5 - 10 g optically clear and polished sections both $AgGaS_2$ and $AgGaSe_2$ were sealed in evacuated fused quartz ampoules with care taken that they not touch. Ampoules were then subjected to elevated temperatures in a near-isothermal furnace for fixed amounts of time, typically overnight but varying from 4 hours to two days. The annealing temperature was initially chosen to be 300°. After the heat treatment cycle, the $AgGaS_2$ was microscopically examined in-situ for signs of surface chemical reaction. After examination, the annealing temperature was increased 50°C and the process was repeated. The procedure was carried out up to 750°C which is 100° below the point where a possible two phase, liquid plus solid region might be expected to occur on the surface of one or both crystals.

The $AgGaS_2$ crystals were afterward removed from the quartz reaction ampoules, polished on the sides so that the reaction surfaces could be inspected in profile, and studied by optical microscopy.

Results

No reaction was observed until an annealing temperature of 600°C was reached, at which time patchy and slightly reddish areas were observed on the surface of the $AgGaS_2$ crystals. The $AgGaSe_2$ crystals remained shiny but developed localized vapor etch pits. At a reaction temperature of 750°C, overall surface roughness and a pronounced reddish surface was observed on the $AgGaS_2$. Surface reaction was obviously occurring probably through the reaction of selenium vapor or Ga_2Se_3 with the $AgGaS_2$ crystal.

Polishing and inspecting the $AgGaS_2$ crystals normal to the reaction surface did not reveal a noticeable grade in color which would indicate a change in the band edge, although rounding of the edges due to polishing might have obscurred the effect if it had occurred to only a very shallow depth.

Discussion

At this time, only very tentative conclusions can be drawn. A coating on the surface of pure $AgGaS_2$ has been observed. This will have to be studied in more detail by optical methods to determine if it is a solid solution between $AgGaS_2$ and $AgGaSe_2$, or a deposited layer of selenium or Ga_2Se. (Both possibilities could account for the results found so far and dispersive analysis or electron beam microprobe analysis can not be used to distinguish.) Further evaluation of these samples is planned using an evaporated gold film followed by mechanical angle lapping to determine if any compositionally graded material was in fact produced.

V. OVERALL CONCLUSIONS AND RECOMMENDATIONS

At the conclusion of this program, one can say that certain aspects were successful, but the major goal of growing $AgGaS_2$ single crystal fibers was not achieved. The partially supported work done to ellucidate the optical defects and the effects of post growth heat

treatment on the optical properties of $AgGaS_2$ (Appendix I) has been a major advance in making this material an important nonlinear optical material. The exploratory attempts to grow this crystal in the form of oriented submillimeter optical quality rods have convinced us that this is not a fruitful direction for future research efforts. Rather, the planar waveguide configuration may be a more useful structure to pursue, since it will allow an extra degree of freedom for angle tuning. A partial success would be the demonstration of thin films of mixed $AgGaS_{2-x}Se_{2x}$ crystals, once this has been confirmed by optical and microchemical studies. That being the case, an important beginning toward IR optical waveguiding in nonlinear media will have been made.

For future research, a serious effort to study interdiffusion in $AgGaS_2$ and $AgGaSe_2$ would seem justified. Both surface reaction through the vapor phase, and solid-state diffusion through conventional mechanical couples would be appropriate in the initial stages of study.

VI. REFERENCES

1. C. H. L. goodman, "Devices and Materials for 4 μm-Band Fibre-Optical Communication," Solid-State and Electron. Devices 2 (1978) 129.

2. A. L. Gentile, M. Braunstein, D. A. Prinnow, J. A. Herrington, D. M. Henderson, L. M. Hobrock, J. Moyer, R. C. Pastor, and R. R. Turk, in "Giber Optics," Ed. B. Bendow and S. S. Mitra, Plenum Press (1979), p. 105-118.

3. D. Chen, R. Skogman, E. Bernal, and C. Butter, in "Fiber Optics," Ed. B. Bendow and S. S. Mitra, Plenum Press (1979), p. 119-124.

4. T. J. Bridges, J. S. Hasiak and A. R. Strnad, "Single-Crystal AGBr Infrared Optical Fibers," Optics Letters 5 (1980) 85.

5. Y. Mimura, Y. Okamura, Y. Komazawa and C. Ota, "Growth of Fiber Crystals for Infrared Optical Waveguides," Japanese J. Appl. Phys. 19 (1980) L269.

6. S. R. Sashital and A. L. Gentile, J. Crystal Growth 69 (1984) 379.

7. S. R. Sashital, J. Crystal Growth 71 (1985) 33.

8. T. J. Bridges, J. S. Hasiak and A. R. Strnad, Optics Lett. 5 (1980) 85.

9. J. C. Mikkelsen and H. Kildal, J. Appl. Phys. 49 (1978) 426.

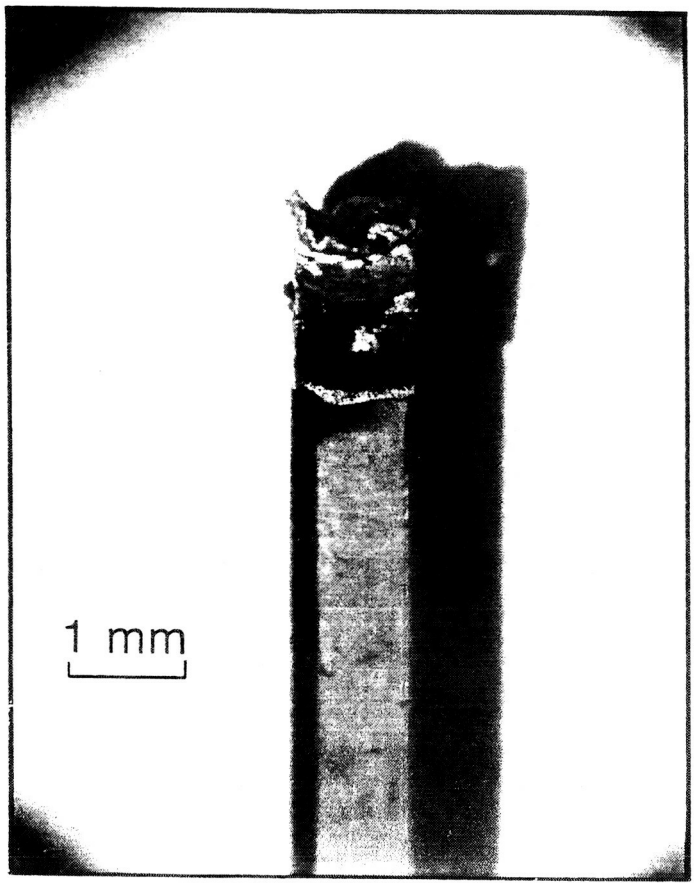

Fig. 1: Photomicrograph of solidified $AgGaSe_2$ feed rod used for direct fusion experiment in the LHPG apparatus. Dark, metallic material at the top indicates loss of sulfur from melt.

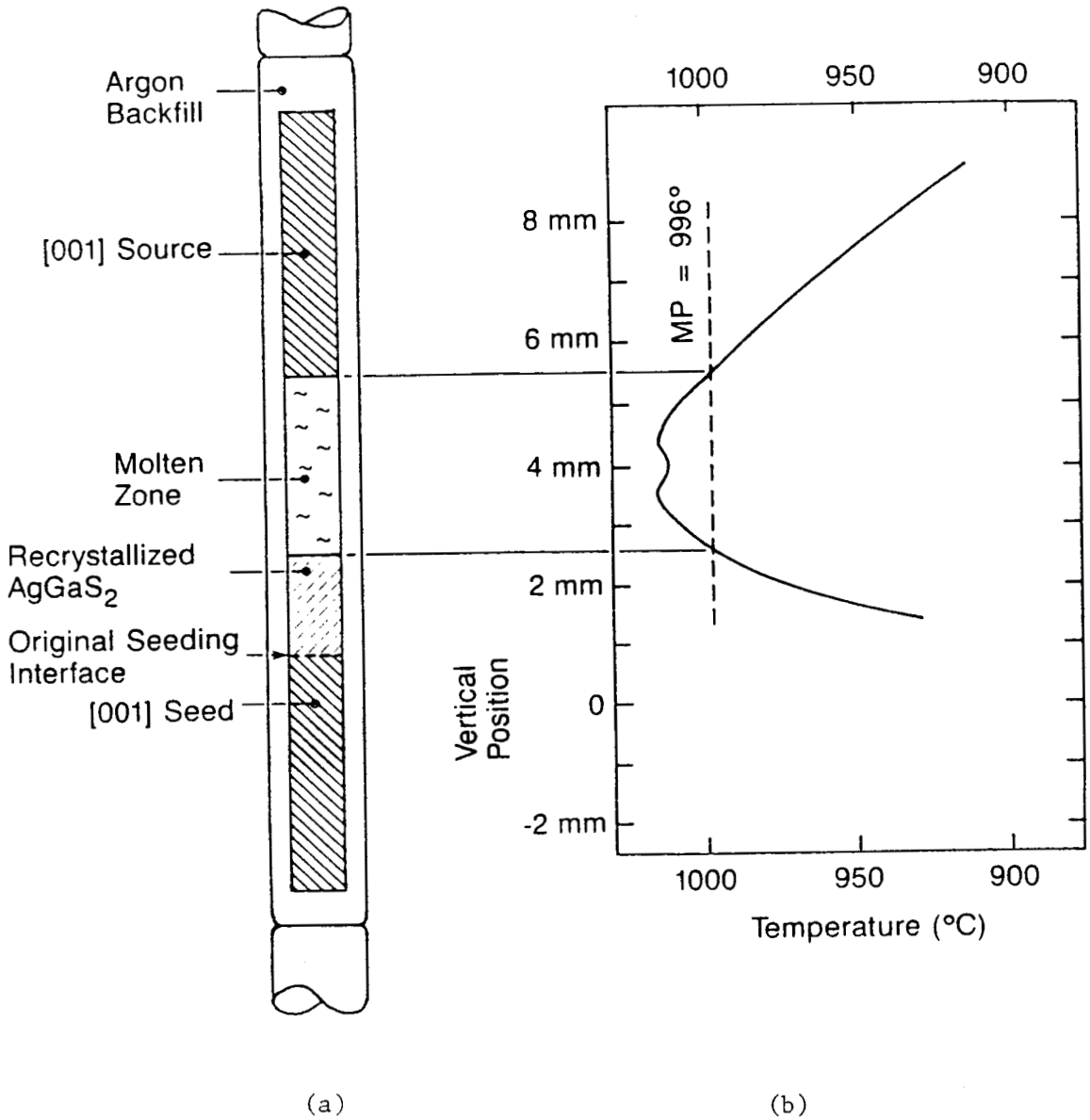

Fig. 2: (a) Melt growth, capillary configuration using centerless-ground 1 mm diameter feedstock. (b) Thermal profile of melt growth furnace.

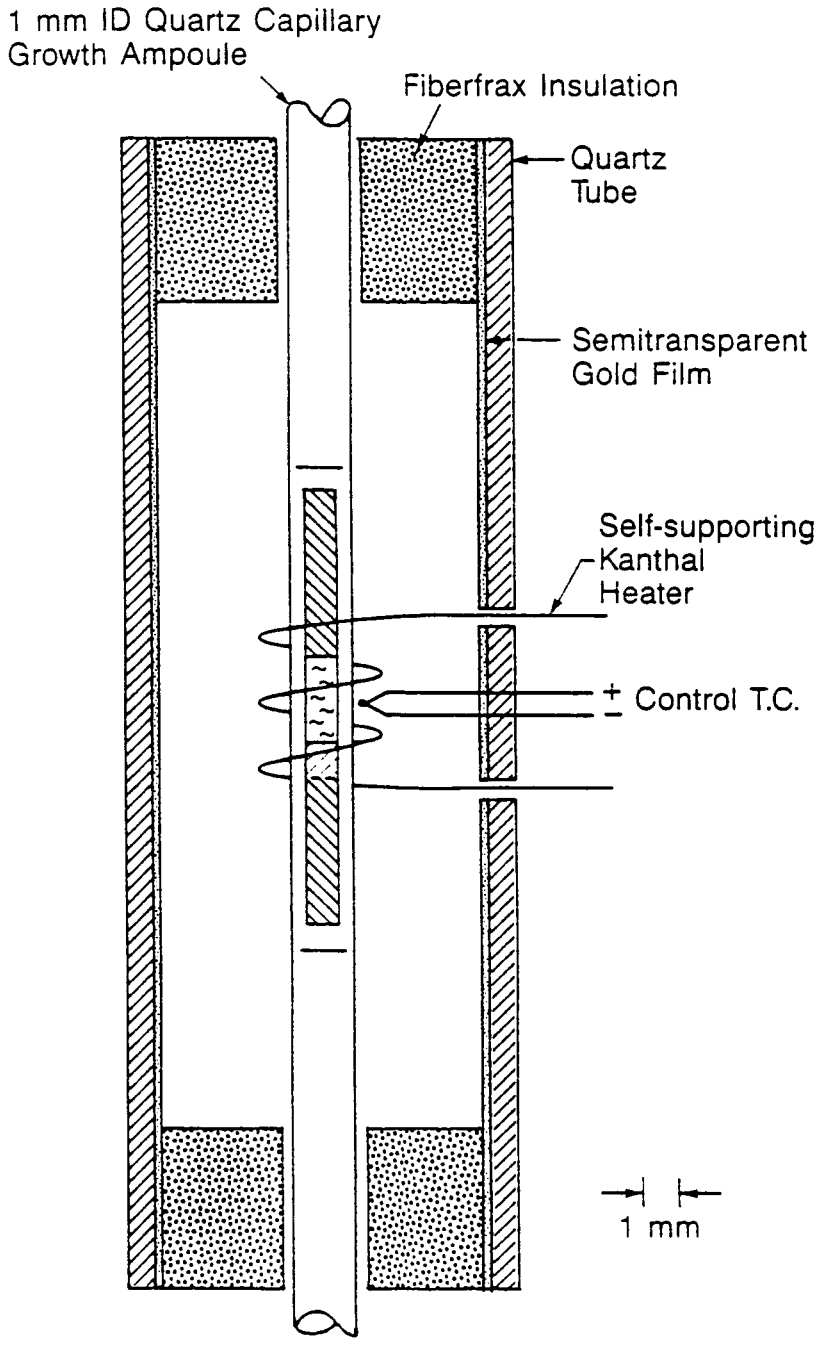

Fig. 3: Configuration of melt growth furnace.

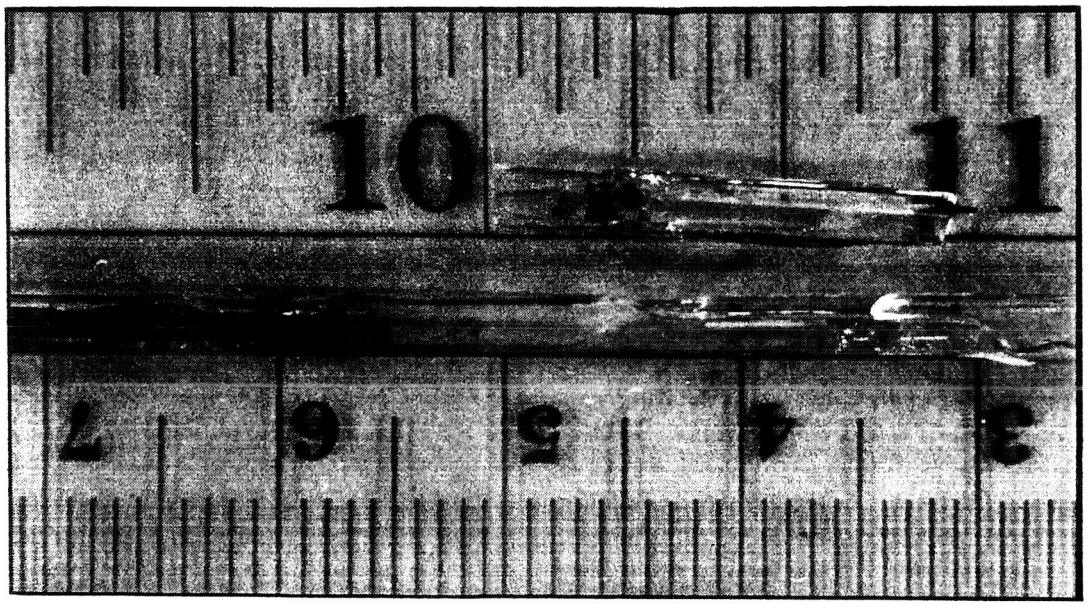

Fig. 4 (a): Photomicrograph of the fused quartz capillary after melt growth experiment. Extensive cracking of the capillaries was encountered.

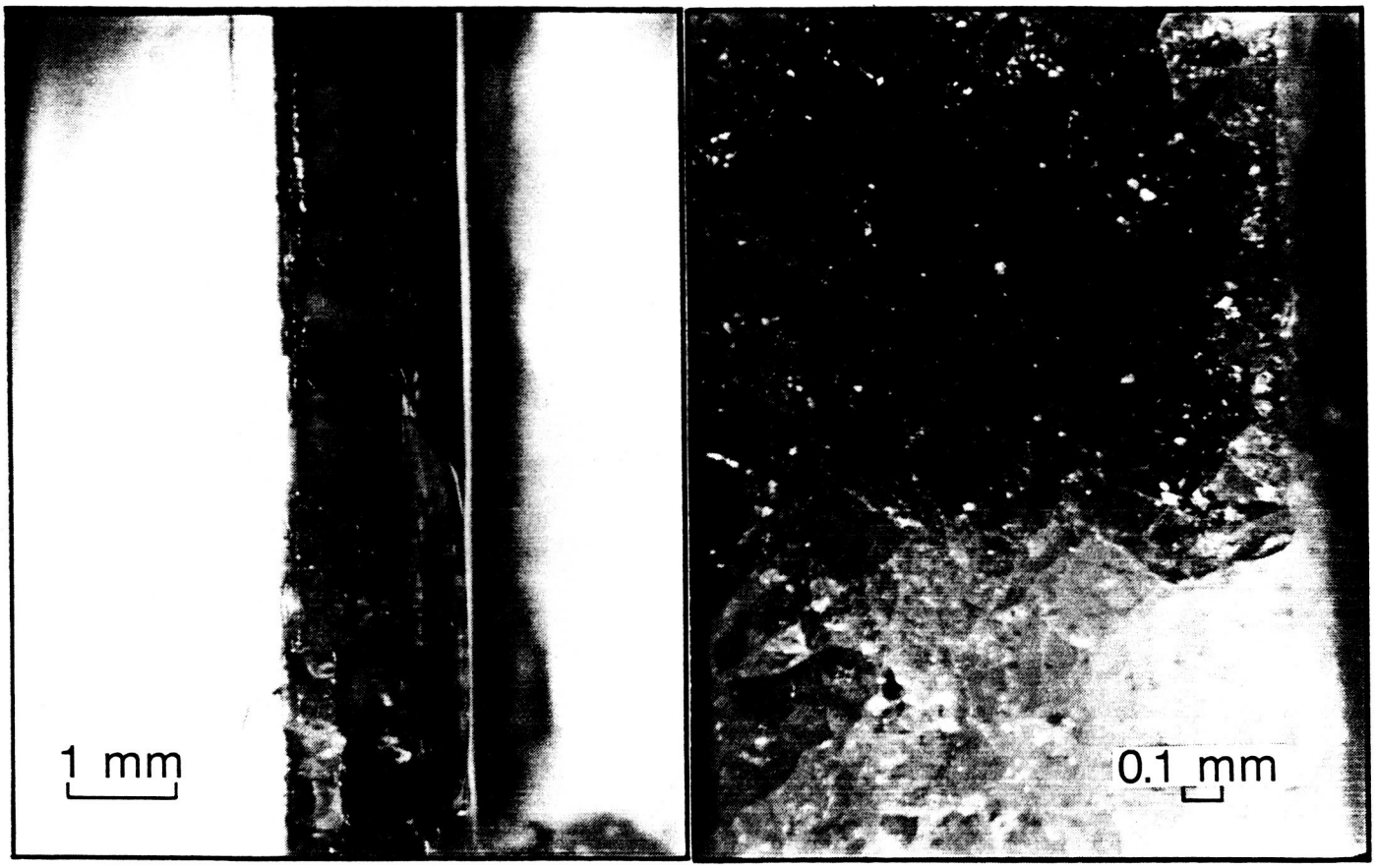

(b) (c)

Fig. 4: (b) Micrograph of capillary showing black, sulfur-deficient material and many total voids. (c) Micrograph of resolidified $AgGaS_2$ showing extensive cracking due to mechanical interaction with the capillary walls.

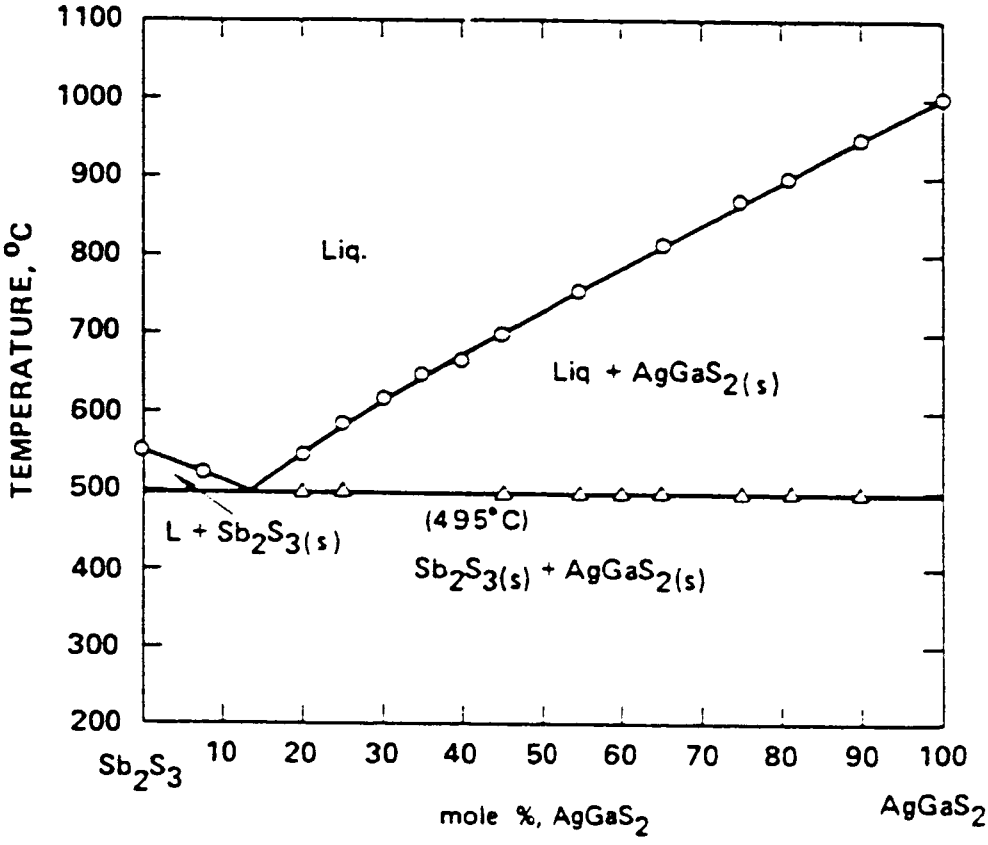

Fig. 5 (a): Phase equilibria in the Sb_2S_3-$AgGaS_2$ pseudobinary system (6).

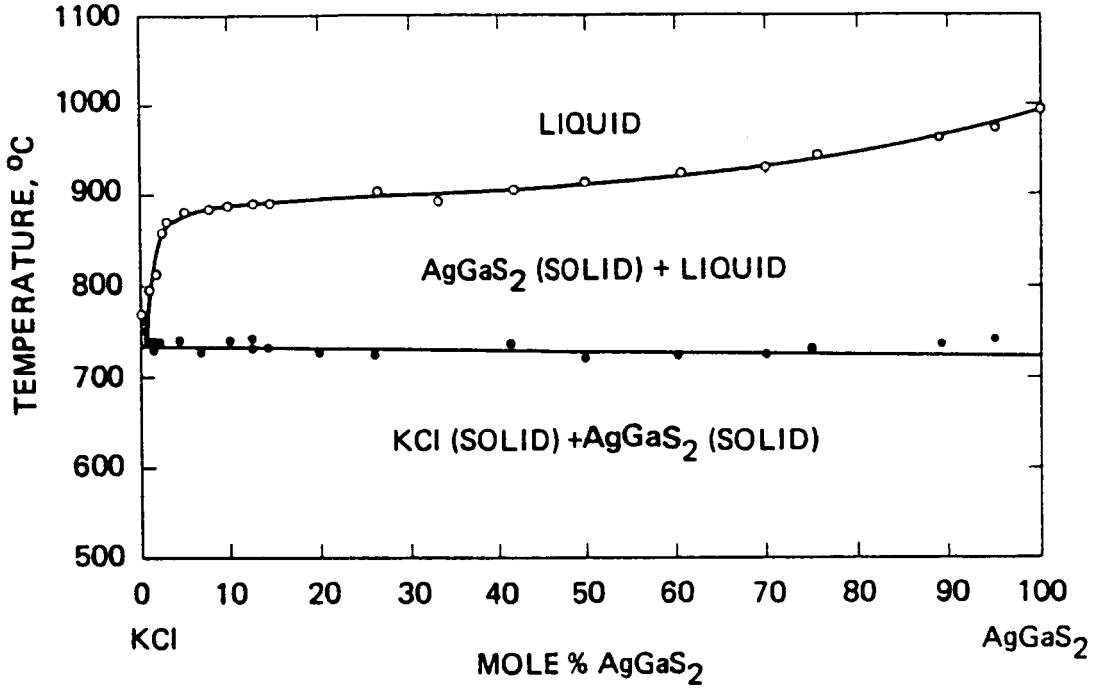

Fig. 5 (b): Phase equilibria in the KCl-$AgGaS_2$ pseudobinary system (7).

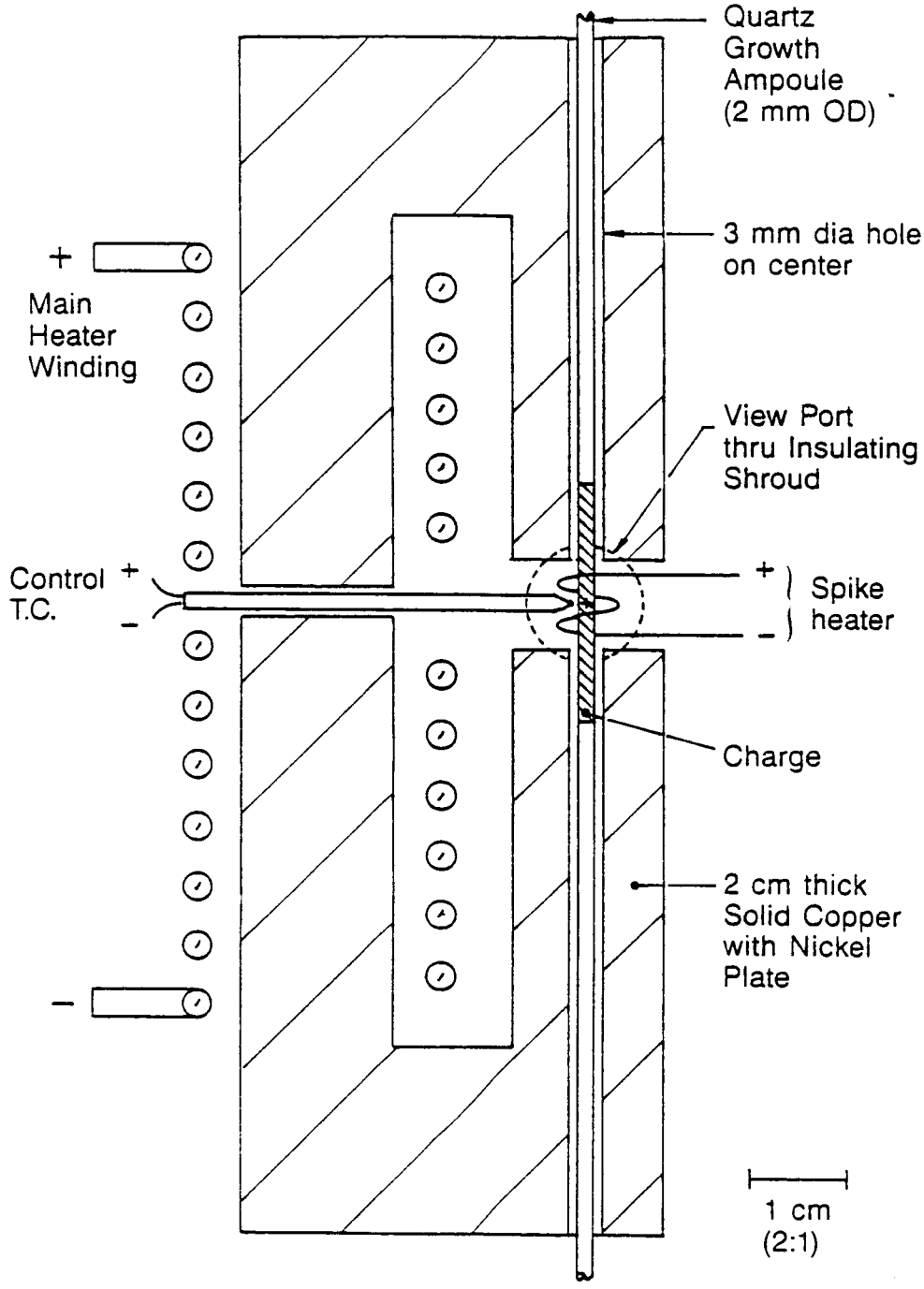

Fig. 6: Configuration of flux growth furnace.

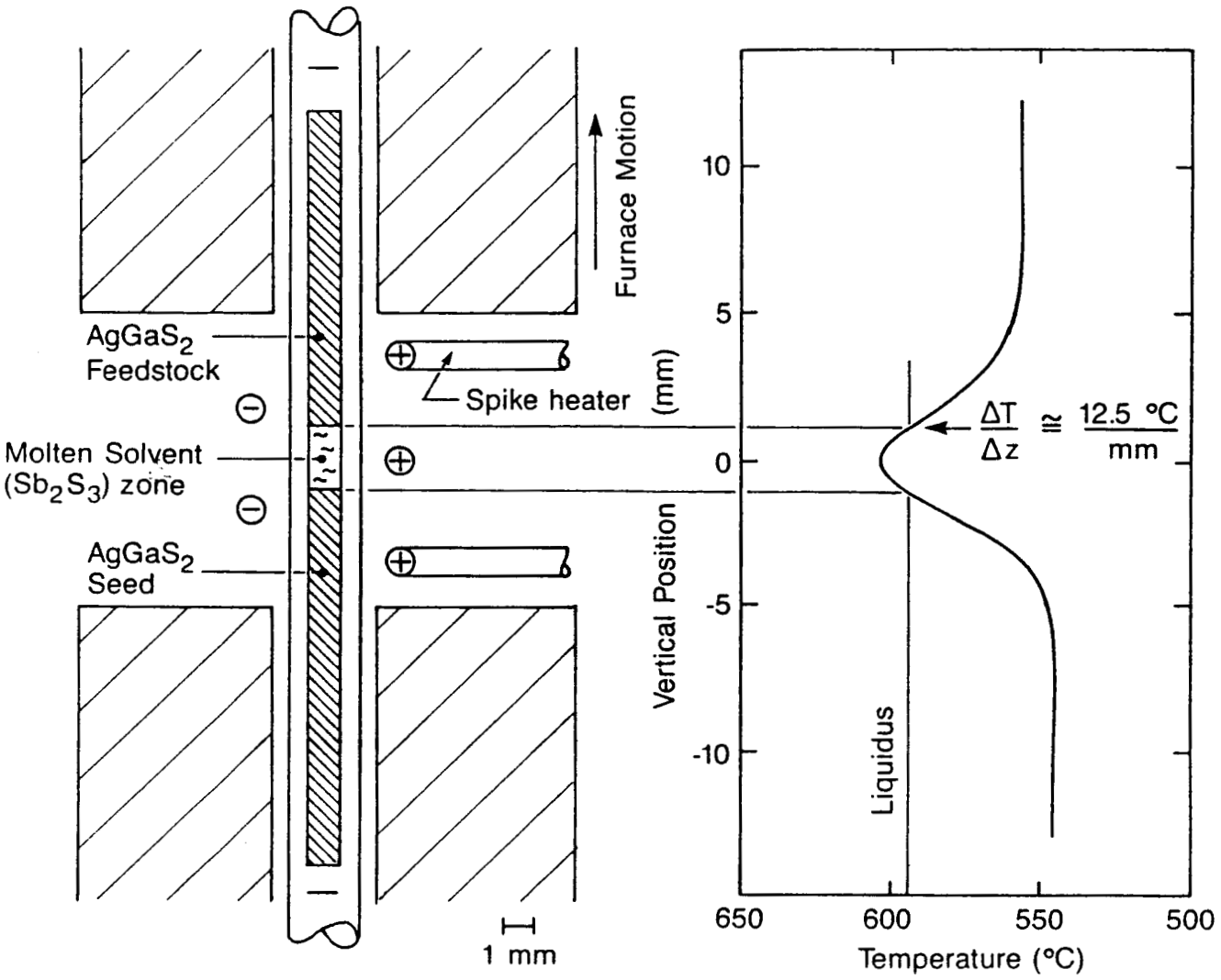

Fig. 7: (a) Details of flux growth furnace system showing: a) The charge with a molten solvent zone. (b) The thermal profile in the capillary.

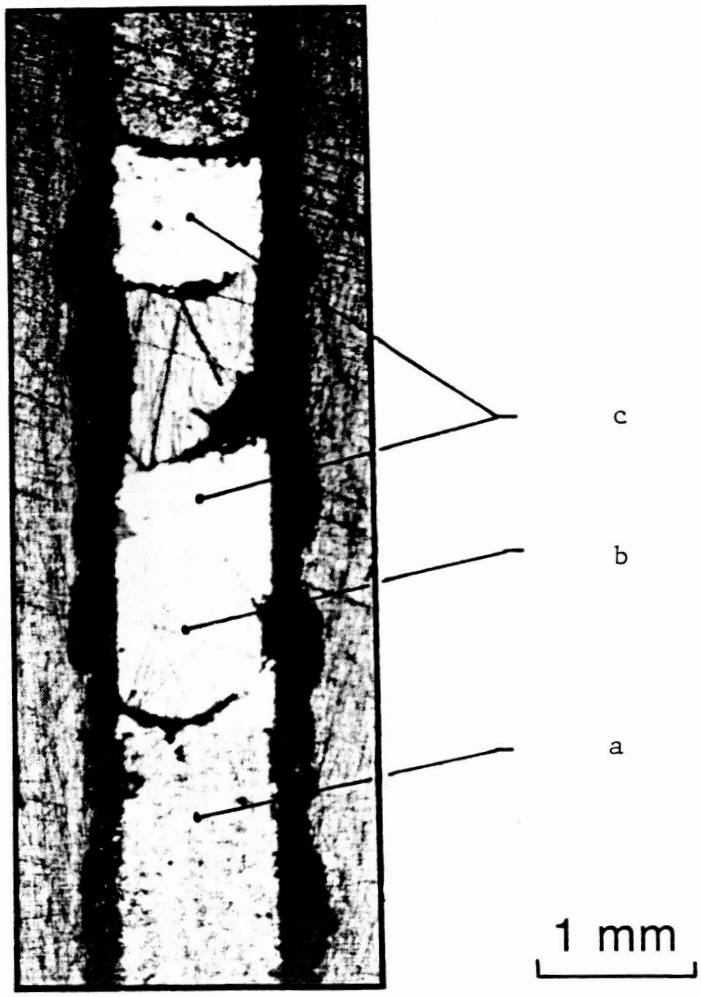

Fig. 8: Cross section of flux growth capillary showing: a) unreacted feedstock, b) solidified Sb_2S_3 solvent, and c) total voids.

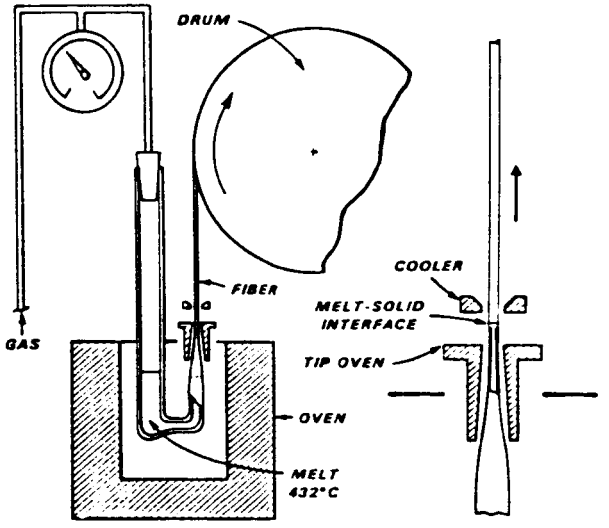

Fig. 9: Schematic diagram of capillary-fed fiber growth apparatus from Bridges et al., OPTICS LETTERS, 5, 85 (1980).

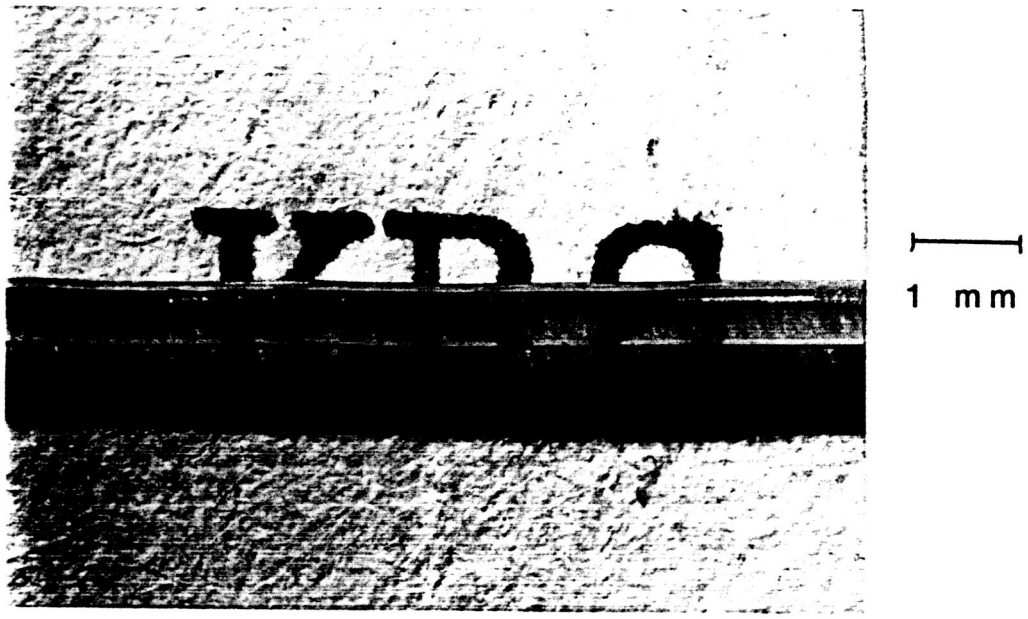

Fig. 10: KRS-5 fiber in incident light showing good diameter uniformity and surface smoothness.

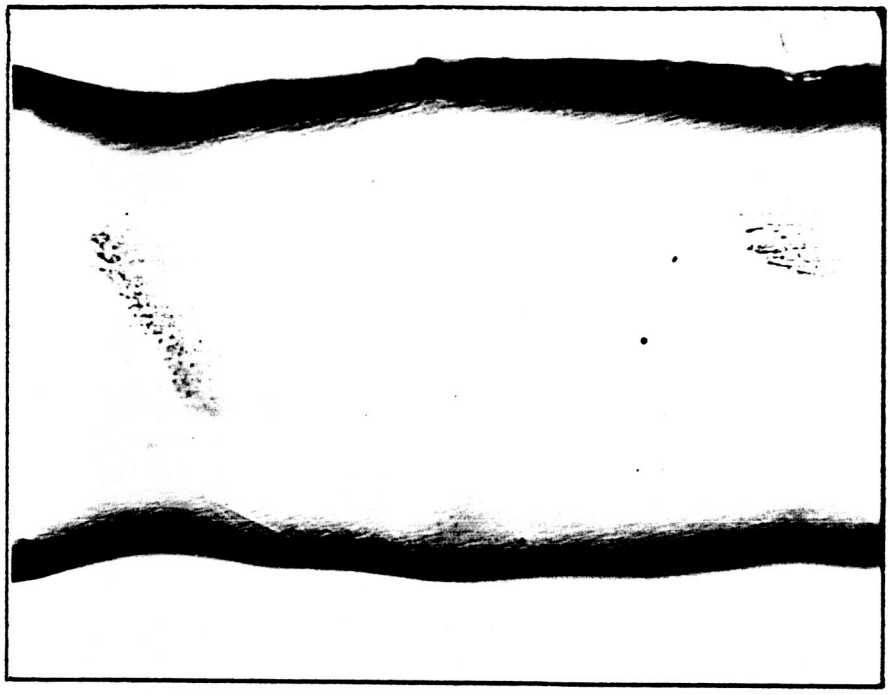

0.1 mm

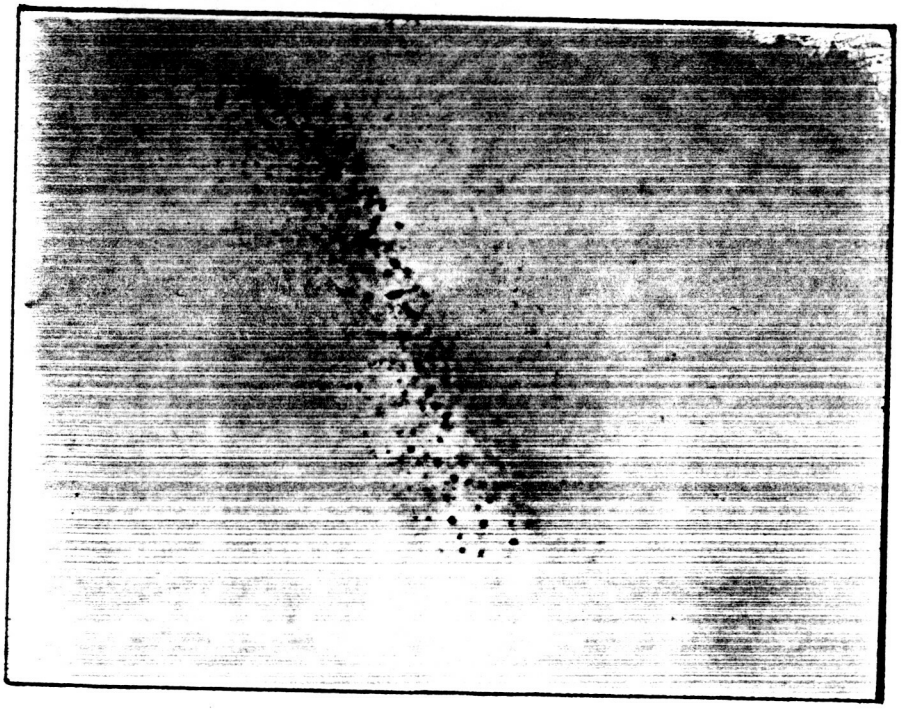

0.1 mm

Fig. 11: Longitudinal thin section of KRS-5 fiber showing the occurrence of defects that appear as voids. They tend to occur whenever there is a sharp "necking in" of the fiber diameter.

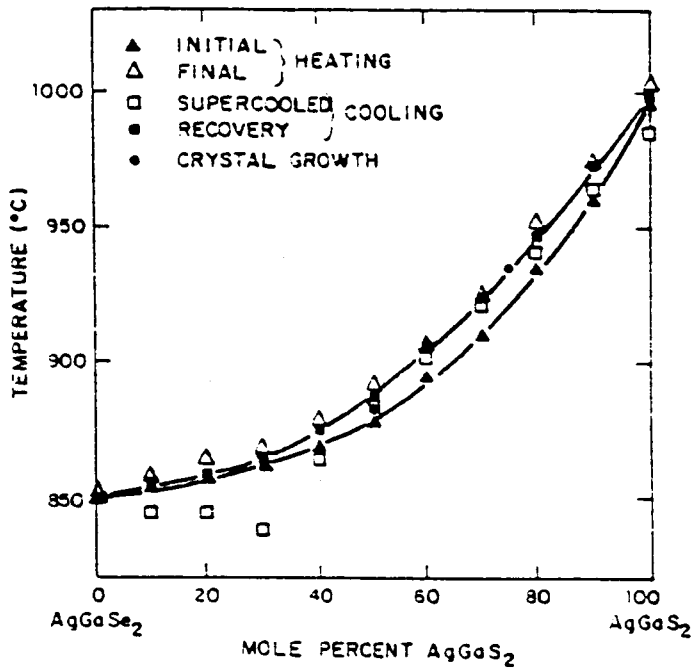

Fig. 12: Phase equilibria in the $AgGaSe_2$-$AgGaS_2$ pseudobinary system in which a complete series of solid solutions exists (9).

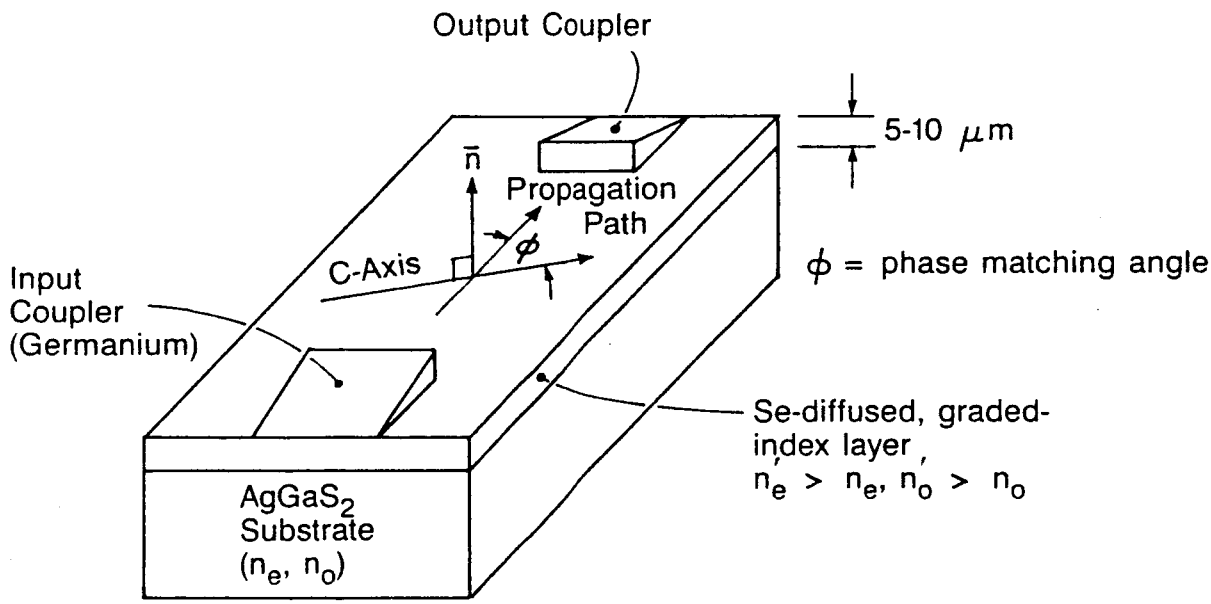

Fig. 13: Thin film, IR waveguiding structure fabricated from a selenium-substituted thin film on an $AgGaS_2$ substrate.

APPENDIX I

Recent developments in the growth of chalcopyrite crystals for nonlinear infrared applications

R. S. Feigelson
R. K. Route
Stanford University
Center for Materials Research
105 McCullough Building
Stanford, California 94305-4045

Abstract. Improvements in crystal growth technology have made it possible to grow crack- and twin-free boules of $AgGaS_2$ and $AgGaSe_2$ in comparatively large dimensions, $AgGaS_2$ to 28 mm diameter by 100 mm length and $AgGaSe_2$ to 37 mm diameter by 100 mm length. Although the crystals grow with optical defects (micrometer-size scattering centers), postgrowth heat treatment procedures have been used to successfully eliminate the defects and produce material of near-theoretical transparency. High optical quality, oriented single crystals of $AgGaS_2$ 1 cm in cross section and more than 2 cm in length and of $AgGaSe_2$ 1 cm in cross section and more than 3.5 cm in length have been produced and are leading to new advances in IR frequency generation. The optical and phase equilibrium studies as well as details of the crystal growth technology that led to this advance in materials technology are described.

Subject terms: optical materials; nonlinear optics; infrared frequency generation; silver thiogallate ($AgGaS_2$); silver selenogallate ($AgGaSe_2$).

Optical Engineering 26(2), 113-119 (February 1987).

CONTENTS

1. INTRODUCTION

Silver thiogallate ($AgGaS_2$) and silver selenogallate ($AgGaSe_2$) are among the I-III-IV_2 compounds that crystallize in the chalcopyrite structure. It was shown more than 10 years ago that these two materials have unique nonlinear infrared optical properties.[1-5] Both are highly nonlinear, and both can be phase matched through relatively large portions of their transparency ranges. $AgGaS_2$ is transparent from 0.45 to 13 μm and can be phase matched for second-harmonic generation (SHG) for fundamental wavelengths between 1.8 and 11 μm. Three-wave mixing processes extend this range somewhat. $AgGaSe_2$ is transparent from 0.73 to 17 μm and can be phase matched for SHG for fundamental wavelengths from 3.1 to 13 μm. Three-wave mixing processes are possible in this material for wavelengths as short as 1.2 μm. Free-carrier absorption is negligible since both materials are semi-insulating. Although reports of their use in nonlinear optical applications have appeared in the literature throughout the past 15 years,[6-13] their full potential has never been realized due to challenging problems in crystal growth and control of optical quality.

Invited Paper OM-108 received Oct. 1, 1986; accepted for publication Dec. 8, 1986; received by Managing Editor Dec. 12, 1986. This paper is a revision of Paper 567-02, which was presented at the SPIE conference on Advances in Materials for Active Optics, Aug. 22-23, 1985, San Diego, Calif. The paper presented there appears (unrefereed) in SPIE Proceedings Vol. 567.

2. BACKGROUND

The compounds $AgGaS_2$ and $AgGaSe_2$ are reactive and somewhat volatile at their melting points (MPs) of 996 °C and 856 °C, respectively. Hence, both must be grown in sealed quartz growth ampoules. Their chalcopyrite structure, space group $\bar{4}2m$, is based upon the zinc blende structure of the III-V group but has lower symmetry due to alternate ordering in the cation sublattice. The unit cell is tetragonal, as shown in Fig. 1, and mechanical and optical properties are different in directions parallel to and normal to the optic axis, or c-axis.

Initial crystal growth experiments on these two materials revealed a number of problem areas, including (1) crystal and ampoule cracking, (2) bands of inclusions, (3) compositional grading, (4) twins, and (5) poor optical quality.[14-18] The crystals had a milky appearance due to a high density of micrometer-size scattering centers.[5,14-16,18-21]

One of the most important discoveries leading to the successful growth of these materials was that by Korczak and Staff,[18] who found that $AgGaS_2$ has anomalous thermal expansion behavior and actually expands along the c-axis as it cools. Iseler[13] later showed that this was true for $AgGaSe_2$ as well. These expansion curves are plotted in Fig. 2. The second important advance was in developing a heat-treatment procedure that was effective in eliminating the scattering centers in as-grown crystals. This was first shown by Matthes et al.[19] for $AgGaS_2$ and by Route et al.[22] for $AgGaSe_2$. The current highly successful crystal growth technology is based on the early work in these two areas.

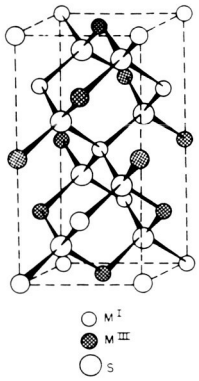

Fig. 1. Unit cell of the chalcopyrite structure.

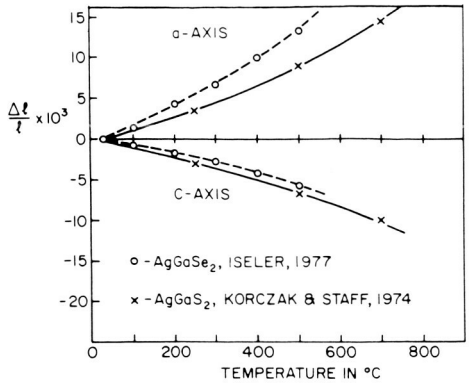

Fig. 2. Thermal expansion properties showing anomalous behavior along the optic axis, or c-axis.

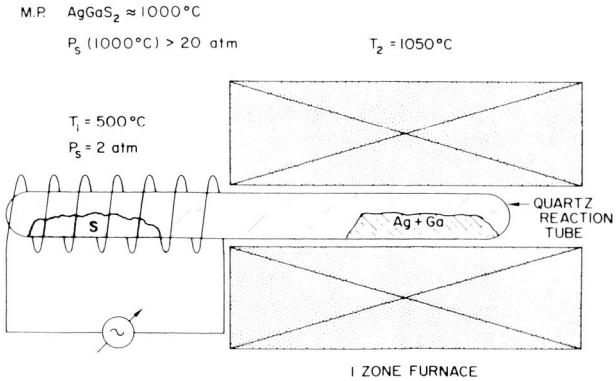

Fig. 3. Vapor transport method for the synthesis of $AgGaS_2$, which prevents rupture of the quartz ampoule. When reaction is complete, the entire ampoule is raised to 1050°C and agitated to achieve homogenization.

3. CRYSTAL GROWTH TECHNOLOGY

3.1. Materials synthesis

Both $AgGaS_2$ and $AgGaSe_2$ melt congruently, and some details of the phase equilibria in both systems along the pseudobinary Ag_2S-Ga_2S_3 and Ag_2Se-Ga_2Se_3 joins are known.[23,24] The compounds are typically made by reaction of high-purity, 99.999% or better, starting materials in elemental form in a separate procedure. In our work we have studied compositions close to stoichiometric. Chemical reaction is carried out in evacuated and sealed fused-quartz ampoules that are internally coated with carbon by pyrolysis of an organic vapor. Because the vapor pressure over elemental sulfur exceeds the rupture strength of fused-quartz ampoules at well below reaction temperature, a two-temperature vapor transport procedure is used to react $AgGaS_2$, as show in Fig. 3. Elemental Se has much lower vapor pressures, so chemical reaction by direct fusion can be used for $AgGaSe_2$. In both cases, we harvest a polycrystalline charge that is highly cracked and shows evidence of compositional variations (this is now known to be unavoidable). The material is then finely broken to achieve some degree of homogenization before it is used as a charge for crystal growth.

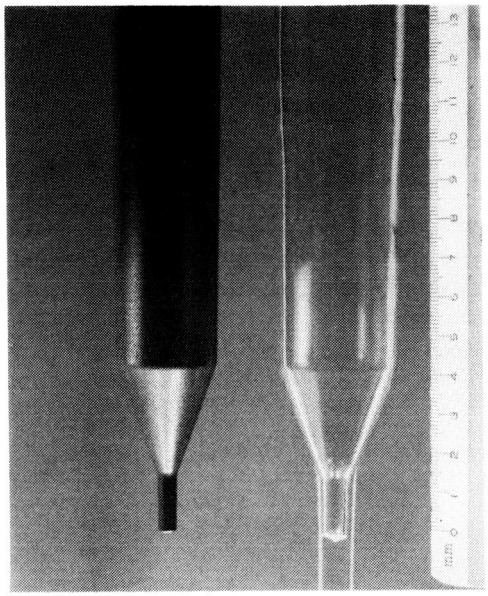

Fig. 4. Precision tapered graphite mandrel and vacuum-formed fused-quartz growth ampoule.

3.2. Crystal growth by the Bridgman method

We have grown crystals by the standard Bridgman-Stockbarger method in a 2½ in. internal diameter (ID) resistance-wound tubular two-zone furnace. Temperature gradients at the growth interface were nominally 18 °C/cm, measured in the open bore. With the growth ampoule present, this was reduced somewhat to 14 °C/cm.

There are two essential features to the successful growth of $AgGaS_2$ and $AgGaSe_2$ in sealed quartz ampoules. First, since the crystals are known to expand along their optic [001] axis during cooling, they must be seeded so that the c-axis is close to the axis of the growth ampoule. (Crystals that nucleate spontaneously typically end up with the c-axis tipped far enough over from the ampoule axis that a net transverse expansion occurs during cooling, with disastrous results.) Second, since c-axis boules expand along their length during cooling, the ampoules must be designed so that mechanical restrictions along their lengths cannot occur. We have solved this problem by designing our fused-quartz growth ampoules with a continuous 1½° taper in both the seed pocket and the main body.

The flare-out region is usually designed with a 20° internal half-angle. Commercial fused-quartz tubing cannot be selected and worked so as to introduce the appropriate taper while maintaining a perfectly round internal cross section. To produce growth ampoules with the desired interior dimensions we have developed a vacuum-forming method by which slightly oversized fused-quartz tubing can be collapsed upon a precision-machined graphite mandrel. Replication of the mandrel surface is exact, and the internal finish is smooth except where machining imperfections on the mandrel surface have occurred. The growth ampoules used in this work were 28 mm ID with a 6 mm diameter by 15 mm long seed pocket and 37 mm ID with an 8 mm diameter by 25 mm long seed pocket. A carbon mandrel and a vacuum-formed ampoule are shown in Fig. 4. Prior to use, the growth ampoules were internally coated with carbon by pyrolysis of an organic vapor.

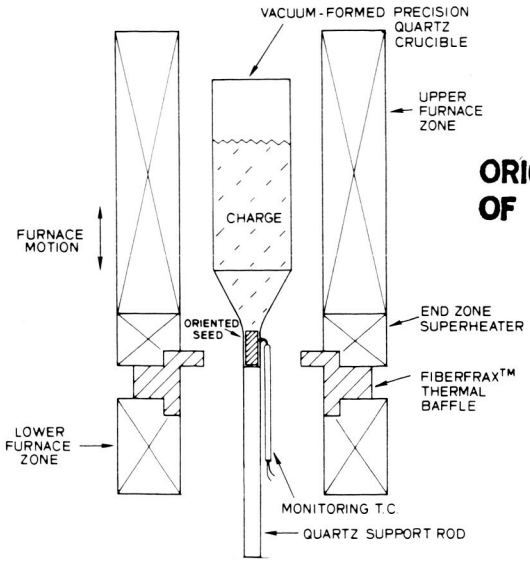

Fig. 5. Bridgman furnace configuration showing thermocouple monitor by which meltback and seed attachment are controlled.

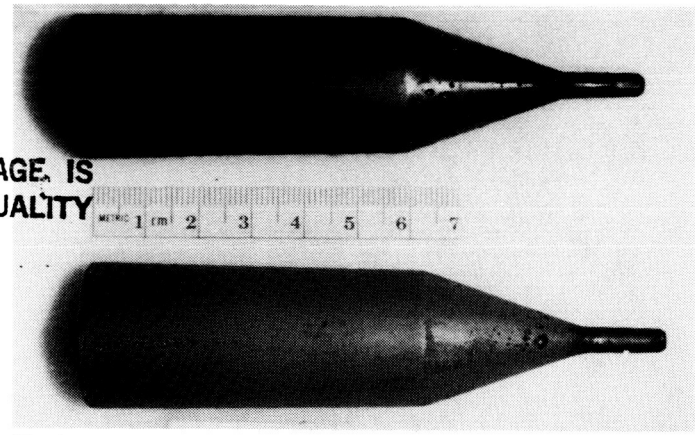

Fig. 6. 28 mm twin- and crack-free boules of $AgGaSe_2$ (top) and $AgGaS_2$ (bottom).

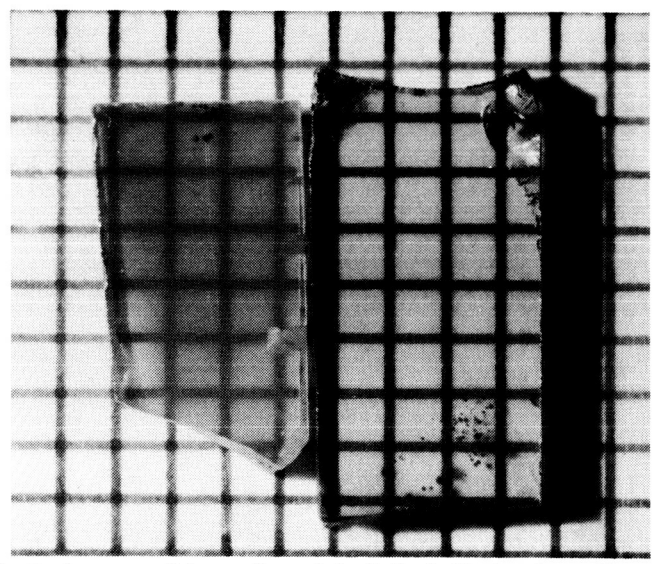

Fig. 7. As-grown thin section of $AgGaS_2$ (left) showing milky appearance compared to clear crystal (right).

Accurately oriented c-axis seeds were hand-fitted to the growth ampoules by a taper grinding method. A few mils' clearance was allowed for transverse thermal expansion during heat-up. Boules were designed to be 10 to 12 cm in length, which required crushed polycrystalline charges of up to 520 g for the 37 mm diameter boules. Prior to sealing, the charged growth ampoules were evacuated to pressures less than 10^{-5} Torr and were then back-filled with 0.5 atmosphere of argon gas purified by passing it through a titanium sponge reactor at 750 °C. Seed attachment was controlled by monitoring a platinum-rhodium thermocouple held against the side of the seed pocket by spring tension. The furnace configuration is shown in Fig. 5. Seeding temperatures, determined empirically, were found to be quite close to the congruent melting points. Crystal growth was then carried out at approximately 15 mm/day. When solidification was complete, the crystals were cooled in the shallow-gradient, lower zone of the furnace at a rate of 50 °C/h.

Properly seeded boules were found to be loose in their ampoules after growth. Occasionally, secondary nucleation on the surfaces was observed. This is thought to be related to failure of the carbon coating. Polycrystalline boules were always seriously cracked due to thermal expansion anisotropy. Minor surface spalling was also occasionally found around localized surface imperfections. In most cases, however, boules remained single and were of excellent structural quality. Refinement of our technique allowed us to grow crystals with very few surface voids. Twins, present in almost all early work, did not occur as long as mechanical interaction with the growth ampoules was carefully prevented. Boules of $AgGaS_2$ and $AgGaSe_2$ free of structural imperfections are shown in Fig. 6. In both cases, compositional variations were observed independent of the charge composition. A thin band of black material always found on the top of $AgGaS_2$ boules was determined by dispersive analysis to be Ag and S rich and was assumed to be Ag_9GaS_6. When charges were made with $\pm 1\%$ excess Ag_2S around the stoichiometric composition, Ag and S rich material was always rejected from the melts. Similar behavior was found for $AgGaSe_2$.

4. OPTICAL PROPERTIES

Although structurally perfect, the as-grown crystals of both $AgGaS_2$ and $AgGaSe_2$ were always found to have a milky appearance. This can readily be seen in the case of $AgGaS_2$, Fig. 7, which is transparent at visible wavelengths. It can also be seen in $AgGaSe_2$ in thin section or with a commercial infrared image converter.

4.1. Microscopic scattering centers

Microscopic examination of $AgGaS_2$ in transmitted light reveals micrometer-wide linear defects, approximately 100 μm long, oriented along the [100] and [010] directions (Fig. 8). Korczak and Staff[18] referred to them as microcracks, which is exactly how they appear. More extensive metallographic preparation and optical microscopic evaluation were carried out in our laboratory, primarily on $AgGaS_2$. The defects were found to consist of precipitates surrounded by localized strain fields[25,26][Fig. 9(a)]. Careful

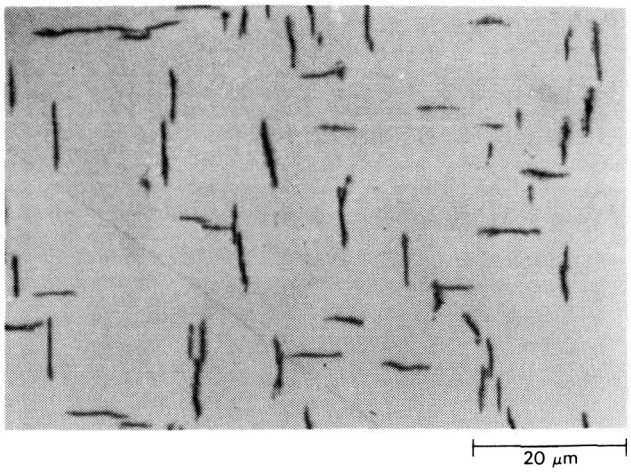

Fig. 8. $AgGaS_2$ viewed along c-axis reveals microscopic scattering defects aligned along the [100] and [010] directions. Their lengths range from 10 to 100 μm, and they have the appearance of microcracks.

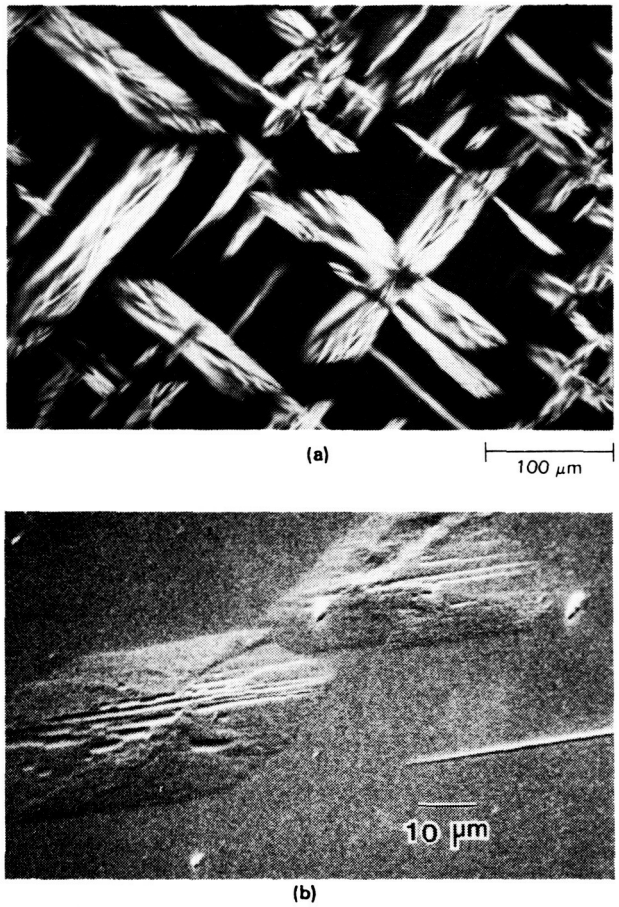

Fig. 9. (a) Microscopic scattering defects and associated strain fields viewed in thin section tilted off the basal plane. A blade-like shape at the core is suggested. (b) Scattering defects are shown to be platelets with a rod-like fine structure lying in the (100) and (010) planes, as revealed by careful polishing and ion-beam milling.

etching and ion-beam milling studies showed that the precipitates are actually 100 μm rectangular platelets lying on the (100) and (010) planes [Fig. 9(b)]. The defects are slightly richer than the matrix in both Ga and S. A corresponding situation is true for the case of $AgGaSe_2$.

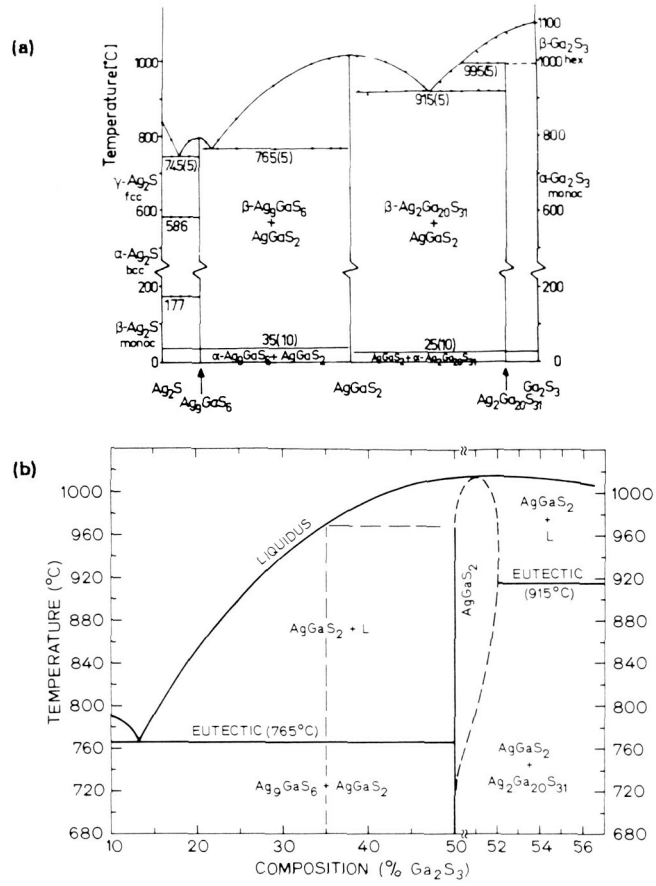

Fig. 10. (a) Pseudobinary Ag_2S-Ga_2S_3 phase diagram of Brandt and Krämer.[23] (b) Proposed phase equilibria suggesting a 2 mole % wide existence region lying entirely on the Ga_2S_3-rich side of stoichiometry.

4.2. Phase equilibrium studies

The precipitates and their surrounding strain fields can be removed from $AgGaS_2$ either by quenching from temperatures above 750 °C or by heat treatment at 900 °C in the presence of Ag_2S.[19,22] To account for these effects, one must understand the thermodynamic phase equilibria along the Ag_2S-Ga_2S_3 pseudobinary join. Differential thermal analysis (DTA) studies on compositions along this join in the vicinity of the stoichiometric composition have been carried out here and elsewhere[23] to ellucidate the detailed nature of the phase equilibria. The DTA technique is quite sensitive. A problem occurs, however, in preparing test samples of precisely determined composition. In-situ synthesis is very difficult because of excessive pressures over any unreacted sulfur, and working from the binary end members is not reliable because Ga_2S_3 exists over a range of compositions.

The maximum melting composition was shown by Brandt and Krämer[23] to lie approximately 1 mole % to the Ga_2S_3-rich side of stoichiometry [Fig. 10(a)] in their study of the complete pseudobinary system. The resolution of our studies was not adequate to reveal additional features near the stoichiometric composition. An existence region of finite width could be inferred from our earlier quenching studies, however, since the compound obviously lies in a single-phase region at temperatures above 750 °C. We therefore conclude that the original phase diagram of Brandt and

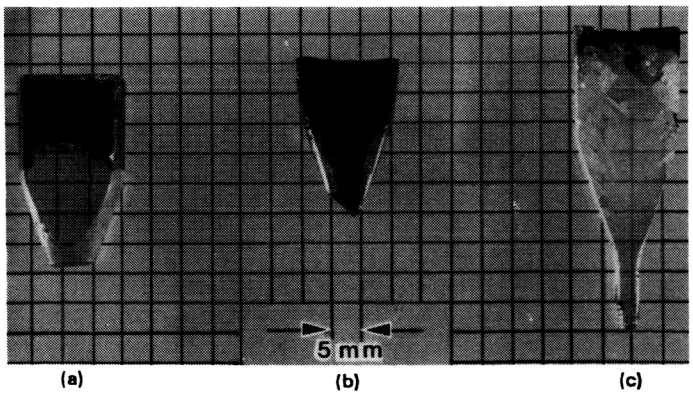

Fig. 11. $AgGaS_2$ crystals grown from solutions rich in Ag_2S. (a) $AgGaS_2$ free of scattering defects was obtained from a solution of composition 65 mole % Ag_2S and 35 mole % Ga_2S_3. (b) 60 mole % Ag_2S; (c) 50 mole % Ag_2S.

Krämer should be modified to include an existence region of approximately 2 mole % width lying entirely on the Ga_2S_3 side of stoichiometry [Fig. 10(b)]. All crystals grown from near-stoichiometric melts will therefore contain excess Ga_2S_3, which precipitates during cooling as an intermediate phase (presumably $Ag_2Ga_{20}S_{31}$) due to retrograde solubility. This model is consistent with our electron microprobe studies of precipitates in $AgGaS_2$ as well as with the tendency of all $AgGaS_2$ boules to reject Ag and S as they grow from stoichiometric melts.

The above model suggests that optically clear material, free of precipitates, might be grown from Ag_2S-rich solutions in which the liquidus temperature is below the point at which the existence region departs from stoichiometry. A series of growth experiments was carried out from Ag_2S-rich solutions, as shown in Fig. 11, to demonstrate this effect. For solutions of greater than 65 mole % Ag_2S, in which the liquidus temperature is in the neighborhood of 960 °C, optically clear crystals were obtained. The method is totally impracticable for the controlled growth of large high quality crystals, however, due to the obvious difficulties in seeding and the need to reject large amounts of material from the growing crystal interface. The growth of high quality but cloudy crystals from congruent melts followed by a heat-treatment procedure turns out to be a far more effective approach.

A totally analogous situation exists for the case of $AgGaSe_2$, and in fact some evidence of a finite width existence region was found by Mikkelsen[24] in his phase equilibrium studies in the Ag_2Se-Ga_2Se_3 system.

4.3. Heat treatment procedures

For $AgGaS_2$, oriented slabs were first cut from as-grown boules. These were then heat treated in a sealed quartz ampoule for 10 to 15 days at 900 °C, according to the procedure shown in Fig. 12, using approximately 0.5 wt. % excess Ag_2S. During this period, Ga_2S_3 or ($2Ga + 3/2S_2$) apparently volatilizes from the surfaces of the crystals and reacts with the excess Ag_2S to form $AgGaS_2$ + liquid (L). Ag and S diffusion causes the bulk crystal to homogenize to a composition on the left-hand boundary of the existence region, very near to stoichiometry, where precipitation due to retrograde solubility does not occur. Optically clear material results, as shown in Fig. 13. A similar process was used for $AgGaSe_2$.

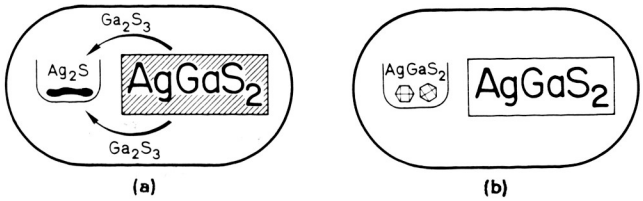

Fig. 12. Postgrowth heat-treatment method (900 °C) used to eliminate optical scattering defects from $AgGaS_2$ crystals. (a) Before; (b) after.

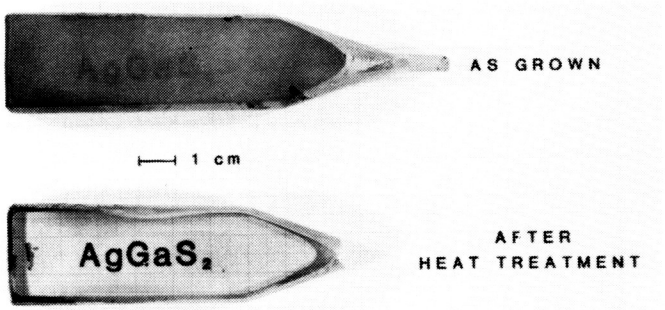

Fig. 13. Comparison of as-grown vs heat-treated $AgGaS_2$ in 11 mm thick sections.

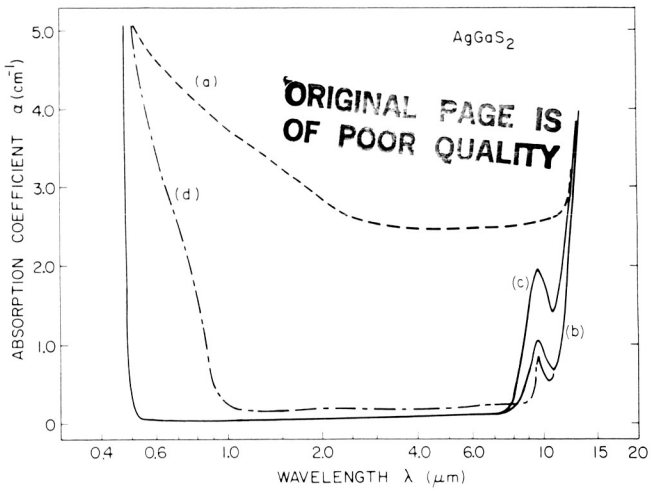

Fig. 14. Spectral absorption of $AgGaSe_2$ (a) as grown, (b) quenched from 900 °C, (c) heat treated with Ag_2S, and (d) heat treated with Ag_2S and then with S.

On occasion, defects were found that could not be removed by repeated heat treatment. These sometimes appeared as negative crystals (internally faceted voids), thought to be caused by the incorporation of additional phases or by the condensation of larger $Ag_2Ga_{20}S_{31}$ precipitates. Their presence, however, does not significantly affect optical transparency. Figure 14 shows transmission measurements made on as-grown, quenched, and heat-treated $AgGaS_2$ crystals. Careful heat treatment resulted in near-theoretical transparency throughout the entire transparency range.

$AgGaS_2$ is useful for nonlinear frequency generation in the 0.5 to 10 μm wavelength range. An intrinsic multiphonon absorption of 0.6 cm^{-1} near 10 μm,[27] however, limits its use for second-harmonic generation of the 10.6 μm line from the CO_2 laser. The reststrahlen bands in $AgGaSe_2$ are located at much longer wavelengths, and this material is

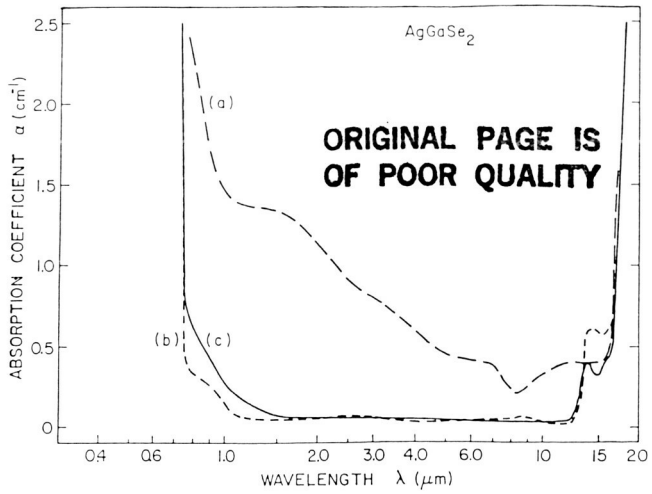

Fig. 15. Spectral absorption of $AgGaSe_2$ (a) as grown, (b) quenched from 650°C, and (c) heat treated with Ag_2Se.

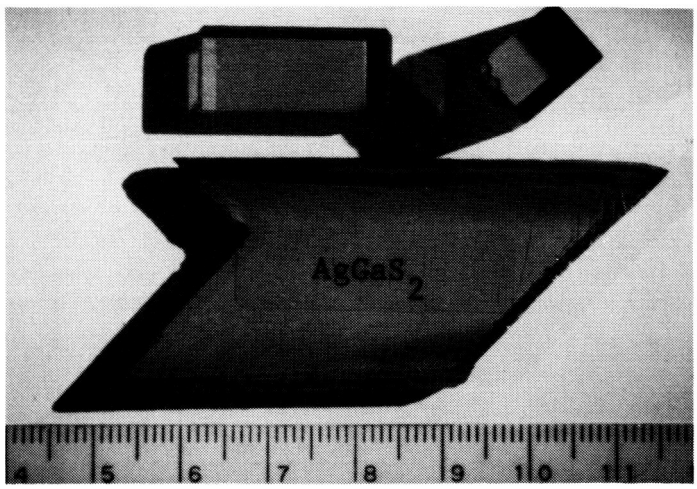

Fig. 16. Fabricated crystals of $AgGaS_2$.

well suited for the application. It, too, was produced as a near-theoretically transparent crystal by an analogous heat-treatment procedure (Fig. 15).

5. OPTICAL CRYSTALS

Using the crystal growth and postgrowth heat-treatment procedures described, we have successfully produced near-theoretically transparent, oriented crystals approximately 1 cm in cross section. The lengths vary slightly depending on the propagation direction, which is determined by the phase-matching conditions. For most experiments it was possible to fabricate $AgGaS_2$ crystals in excess of 22 mm long from 28 mm diameter boules (Fig. 16) and $AgGaSe_2$ crystals in excess of 35 mm long from 37 mm diameter boules. Most crystals are oriented with the propagation direction between 45° and 90° to the boule axis. Because of the anomalous thermal expansion problem, for all useful phase-matching conditions we are prevented from growing the crystals sufficiently close to the propagation direction to harvest substantially longer crystals. To obtain longer interaction lengths, crystals of larger diameter must be grown.

6. RECENT NONLINEAR OPTICAL RESULTS

With the high optical quality, twin-free crystals of both $AgGaS_2$ and $AgGaSe_2$ described, significant advances in nonlinear IR optical technology have been made. Principal among these are the demonstration of optical parametric oscillation in $AgGaS_2$[7,28] and in $AgGaSe_2$[29] and efficient second-harmonic conversion of the carbon dioxide laser.[30] Details of these experiments are included in Table I.

The limitation of both materials is their relatively moderate threshold for surface damage, which is in the 10 to 15 MW/cm^2 range. Preliminary experimentation with various antireflection surface coatings indicated that these values may be raised by a factor of 2 or more, and consequently, higher conversion efficiencies should be possible. The alternative approach is, of course, to grow larger boules from which longer (and hence more efficient) crystals can be obtained.

TABLE I. Results of experiments on $AgGaS_2$ and $AgGaSe_2$.

		References
Parametric oscillation in $AgGaS_2$	pump wavelength: 1.06 μm, 20 ps mode-locked output wavelength: 1.2–10 μm quantum conversion efficiency: 0.1–10%	7
	pump wavelength: 1.06 μm output wavelength: 1.4–4.0 μm threshold: 1.2 mJ peak energy conversion: 16%	28
Difference-frequency generation in $AgGaS_2$	input wavelength: 1.06 μm, tunable dye output wavelength: 5–11 μm	12
	input wavelength: 1.06 μm, tunable dye output wavelength: 3.3–11 μm	31
Second-harmonic generation in $AgGaSe_2$	pump wavelength: 10.25 μm output wavelength: 5.13 μm energy conversion efficiency: 14%	30
Parametric oscillation in $AgGaSe_2$	pump wavelength: 2.05 μm output wavelengths: 2.65–9.02 μm energy conversion efficiency: 18% near degeneracy at 4.1 μm	29
Damage	Surface damage thresholds have been measured at a number of wavelengths. For 20–50 ns pulses they are typically 13 MW/cm^2. Bulk damage thresholds are at least one order of magnitude higher.	28,29,30

7. CONCLUSIONS

The practical problems associated with the growth of high optical quality, twin-free crystals of both $AgGaS_2$ and $AgGaSe_2$ have been resolved. Near-theoretically transparent

crystals 1 cm in cross section and in lengths exceeding 22 mm and 35 mm, respectively, have been produced. With these, useful and practical solid-state nonlinear infrared optical devices have been realized.

8. ACKNOWLEDGMENTS

This work was supported by the National Science Foundation Materials Research Laboratory Program through the Center for Materials Research at Stanford University and by the U.S. Army Research Office, the Office of Naval Research, NASA, SRI International, and Quanta-Ray, Inc. Optical microscopy and photographs by R. Koch.

9. REFERENCES

1. D. S. Chemla, P. J. Kupecek, D. S. Robertson, and R. C. Smith, "Silver thiogallate, a new material with potential for infrared devices," Opt. Commun. 3(1), 29-31 (1971).
2. G. D. Boyd, H. Kasper, and J. H. McFee, "Linear and nonlinear optical properties of $AgGaS_2$, $CuGaS_2$, and $CuInS_2$, and theory of the wedge technique for the measurement of nonlinear coefficients," IEEE J. Quantum Electron. QE-7(12), 563-573 (1971).
3. G. D. Boyd, H. M. Kasper, J. H. McFee, and F. G. Storz, "Linear and nonlinear optical properties of some ternary selenides," IEEE J. Quantum Electron. QE-8(12), 900-908 (1972).
4. H. Kildal and J. C. Mikkelsen, "The nonlinear optical coefficient, phasematching, and optical damage in the chalcopyrite $AgGaSe_2$," Opt. Commun. 9(3), 315-318 (1973).
5. G. C. Bhar and R. C. Smith, "Optical properties of II-IV-V_2 and I-III-VI_2 crystals with particular reference to transmission limits," Phys. Status Solidi. A: 13(1), 157-168 (1972).
6. W. Jantz and P. Koidl, "Efficient up-conversion of 10.6-μm radiation into the green spectral range," Appl. Phys. Lett. 31(2), 99-101 (1977).
7. T. Elsaesser, A. Seilmeier, W. Kaiser, P. Koidl, and G. Brandt, "Parametric generation of tunable picosecond pulses in the medium infrared using $AgGaS_2$ crystals," Appl. Phys. Lett. 44(4), 383-385 (1984).
8. R. L. Byer, M. M. Choy, R. L. Herbst, D. S. Chemla, and R. S. Feigelson, "Second harmonic generation and infrared mixing in $AgGaSe_2$," Appl. Phys. Lett. 24(2), 65-68 (1974).
9. R. J. Seymour and F. Zernike, "Infrared radiation tunable from 5.5 to 18.3 μm generated by mixing in $AgGaS_2$," Appl. Phys. Lett. 29(11), 705-707 (1976).
10. D. C. Hanna, V. V. Rampal, and R. C. Smith, "Tunable infrared down-conversion in silver thiogallate," Opt. Commun. 8(2), 151-153 (1973).
11. D. Frölich, K. Reimann, and P. Koidl, "Investigation of mixed-mode polariton dispersion in $AgGaS_2$," Phys. Status Solidi. B: 114(2), 553-559 (1982).
12. K. Kato, "High-power difference-frequency generation at 5-11 μm in $AgGaS_2$," IEEE J. Quantum Electron. QE-20(7), 698-699 (1984).
13. G. W. Iseler, "Thermal expansion and seeded Bridgman growth of $AgGaSe_2$," J. Cryst. Growth 41(1), 146-150 (1977).
14. H. A. Chedzey, D. J. Marshall, H. T. Parfitt, and D. S. Robertson, "A study of the melt growth of single-crystal thiogallates," J. Phys. D: 4(9), 1320-1324 (1971).
15. B. Tell and H. M. Kasper, "Optical and electrical properties of $AgGaS_2$ and $AgGaSe_2$," Phys. Rev. B: 4(12), 4455-4459 (1971).
16. H. M. Kasper, "Crystal growth and properties of some I-III-IV_2 compounds," Nat. Bur. Std.(U.S.) Spec. Publ. 364, 671-679 (1972).
17. P. W. Yu and Y. S. Park, "Sharp-line and broad-band emission in $AgGaS_2$ crystals," J. Appl. Phys. 45(2), 823-827 (1974).
18. P. Korczak and C. B. Staff, "Liquid encapsulated Czochralski growth of silver thiogallate," J. Cryst. Growth 24/25, 386-389 (1974).
19. H. Matthes, R. Viehmann, and N. Marschall, "Improved optical quality of $AgGaS_2$," Appl. Phys. Lett. 26(5), 237-239 (1975).
20. R. K. Route, R. S. Feigelson, and R. J. Raymakers, "Growth of $AgGaSe_2$ for infrared applications," J. Cryst. Growth 24/25, 390-395 (1974).
21. R. K. Route, R. J. Raymakers, and R. S. Feigelson, "Preparation of large untwinned single crystals of $AgGaS_2$ and $AgGaSe_2$," J. Cryst. Growth 29(1), 125-126 (1975).
22. R. K. Route, R. S. Feigelson, and R. J. Raymakers, "Elimination of optical scattering defects in $AgGaS_2$," J. Cryst. Growth 33(2), 239-245 (1976).
23. G. Brandt and V. Krämer, "Phase investigations in the silver-gallium-sulfur system," Mater. Res. Bull. 11(11), 1381-1388 (1976).
24. J. C. Mikkelsen, Jr., "Ag_2Se-Ga_2Se_3 pseudobinary phase diagram," Mater. Res. Bull. 12(5), 497-502 (1977).
25. R. Koch, R. K. Route, and R. S. Feigelson, "Microscopic scattering centers in $AgGaS_2$," Il Nuovo Cimento 2D(6), 1767-1774 (1983).
26. R. S. Feigelson, R. Koch, R. K. Route, and C.-E. Huang, "Defects in the ternary chalcopyrites $AgGaS_2$ and $AgGaSe_2$," in collected abstracts, IOCG VII Int. Conf. on Crystal Growth (Stuttgart) (1983).
27. G. C. Bhar and R. C. Smith, "Silver thiogallate ($AgGaS_2$)—Part II: Linear optical properties," IEEE J. Quantum Electron. QE-10(7), 546-550 (1974).
28. Y. X. Fan, R. C. Eckardt, R. L. Byer, R. K. Route, and R. S. Feigelson, "$AgGaS_2$ infrared parametric oscillator," Appl. Phys. Lett. 45(4), 313-315 (1984).
29. R. C. Eckardt, Y. X. Fan, R. L. Byer, C. L. Marquardt, M. E. Storm, and L. Esterowitz, "Broadly tunable infrared parametric oscillator using $AgGaSe_2$," Appl. Phys. Lett. 49(11), 608-613 (1986).
30. R. C. Eckardt, Y. X. Fan, R. L. Byer, R. K. Route, R. S. Feigelson, and J. van der Laan, "Efficient second harmonic generation of 10-μm radiation in $AgGaSe_2$," Appl. Phys. Lett 47(8), 786-788 (1985).
31. D. S. Bethune and A. C. Luntz, "A laser infrared source of nanosecond pulses tunable from 1.4 to 22 μm," Appl. Phys. B: 40(2), 107-113 (1986).

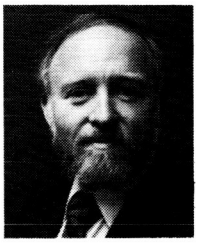

Robert S. Feigelson holds a BS in ceramic engineering from the Georgia Institute of Technology, MS in ceramics from Massachusetts Institute of Technology, and Ph.D. in materials science from Stanford University. For over 20 years he has been involved in single crystal growth and materials preparation. He has a broad range of experience and expertise in both bulk and epitaxial growth processes on a variety of materials ranging from semiconductors to ferroelectric oxides and magnetic materials. Professor Feigelson is involved with both the technical and administrative direction of the Crystal Science Division of the Center for Materials Research as well as his own research. He is engaged in cooperative programs with faculty and students in various departments at Stanford and in joint materials research programs with investigators in the U.S. and internationally.

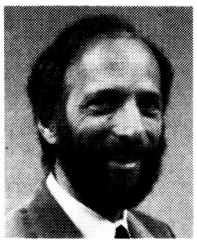

Roger Route holds a BS in electrical engineering from the University of Michigan and MS and Ph.D. degrees in electrical engineering from Stanford University. Since graduating in 1970, he has been employed as a research associate, now at the senior level, at the Center for Materials Research, Stanford University. His area of greatest interest has been the growth and characterization of a variety of crystalline materials. Most recently, the growth of large IR-transmitting semicondictor crystals for nonlinear optical applications and of oxide crystals, transparent in the visible, for laser hosts and nonlinear applications have occupied most of his research efforts. He has authored or coauthored over 30 technical publications in these areas.

APPENDIX II

The most versatile of the melt growth techniques used for fiber growth is the float-zone method. When the fiber diameter is smaller than the source rod diameter from which it grows, as shown in fig. 1, it is also known as pedestal growth. Of all the methods used for melt growth, it alone does not require crucibles for furnace components which can lead to contamination and confinement stress problems. In addition, crystals of congruently and incongruently melting crystals can be grown, and the composition of the crystal can be controlled by controlling the composition of the starting material. With the small crystal size and focussed heat source, steep temperature gradients, and hence rapid growth rates typically on the order of mm/min, can be achieved.

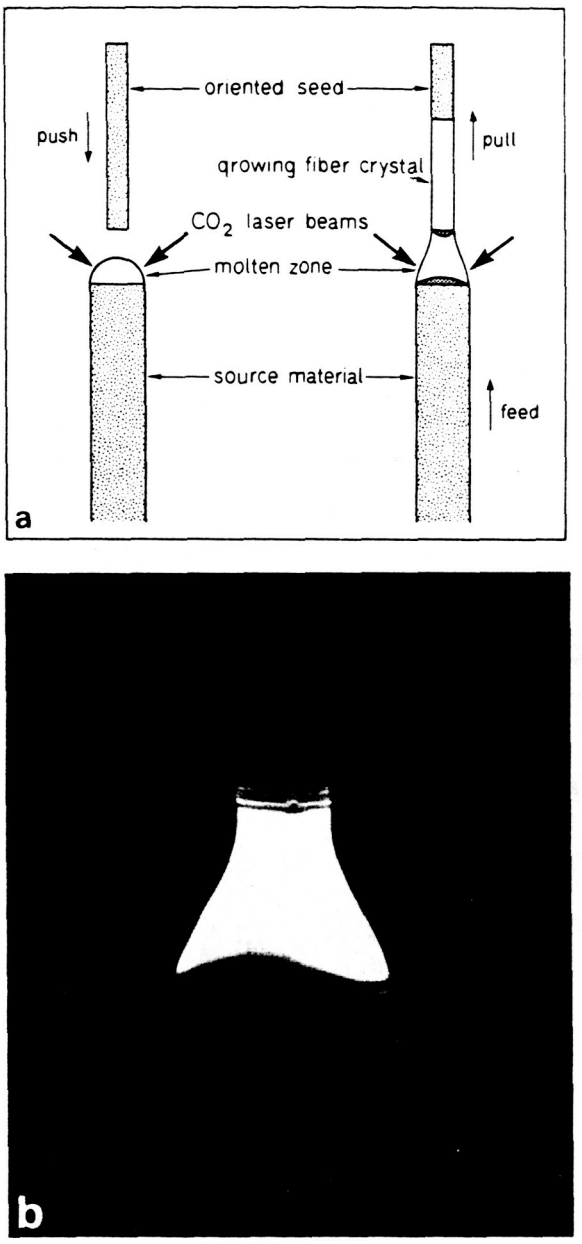

Fig. 1. (a) Schematic diagram of pedestal growth and (b) photograph of an actual $LiNbO_3$ fiber growing by the LHPG method. The larger diameter ground source rod is at the bottom. A growth ridge is clearly visible on the fiber.

There are several types of heat sources which can be used to produce molten zones suitable for use with the pedestal growth method. For fiber growth they must be able to produce zones having dimensions comparable to that of the fiber and source rod diameters. Resistance, induction, electron beam, focused lamp, and laser heating are all possible. It is difficult, however, to produce small zones with steep induction heating requires either a conducting sample or a susceptor and vacuum chamber.

Laser heating is an ideal heat source because it can be tightly focussed directly onto the sample with a beam size comparable with fiber dimensions (which may vary from a few microns to several mm), can be used in ambient, inert, reactive or vacuum atmospheres and is available in power levels which can readily melt any known material whose dimensions are of the order of the beam size. Growth can be achieved by either moving the laser beam or the source rod and fiber.

Because the optical train is cumbersome, it is much easier to move the source rod and seed. In our growth apparatus, a precision ground dovetail combined with two leadscrew drives achieves independent, linear motion of the source rod and seed.

To initiate growth, the top of the source rod is first heated until a small molten button is formed. Then the oriented seed is dipped into the melt and a stable molten zone forms as shown in fig. 1. Growth commences as the seed is slowly withdrawn from the melt and compensating source material fed in from the bottom. Depending upon the relative feed and pull rates, conservation of mass will determine the ratio of fiber diameter to source rod diameter. For most materials, the most stable growth is achieved with the growing fiber being 1/2 to 1/3 the source rod diameter.

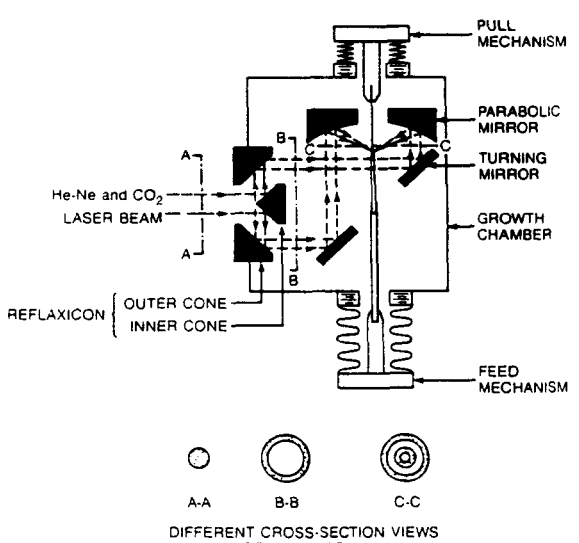

Fig. 2. Schematic diagram of a circularly symmetric laser optical system useful for fiber growth, including (a) optics for circular heating, (b) He-Ne laser for alignment, (c) CO_2 laser for melting the source rod, and (d) different cross-sectional views of laser beams.

Laser power and fiber and source diameters determine the height of the molten zone. Again, for most materials the most stable growth is achieved when the height of the molten zone is approximately $\frac{3}{2}$ the average of the source and fiber diameter. Originally multiple beam laser systems were used, but a new optical system now has been developed which produces a much more uniform, ring shaped beam, as illustrated in fig. 2, eliminating hot spots in the molten zone caused by the multiple beam approach.

Any deviation from a smooth, uniform cylindrical fiber geometry can lead to significant optical losses in fiber devices. Little can be done to eliminate growth anisotropy induced facetting such as that found for c-axis Nd:YAG and a-axis $LiNbO_3$ crystals as shown in fig. 3. This problem

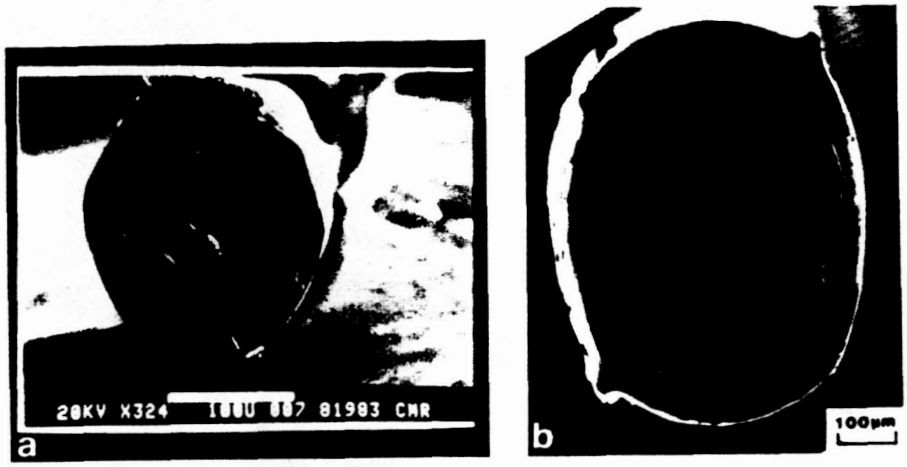

Fig. 3. Cross-sectional facets found in fibers of (a) *c*-axis Nd : YAG and (b) *a*-axis $LiNbO_3$.

is less important, however, than diameter variations arising from poor temperature and zone stability such as that shown in fig. 4a. Both long and short term diameter fluctuations have been encountered during fiber growth, some of which can be eliminated by careful control of temperature, the reduction ratio, the push/pull rates, the diameter uniformity of the source rod, and fiber orientation (fig. 4b).

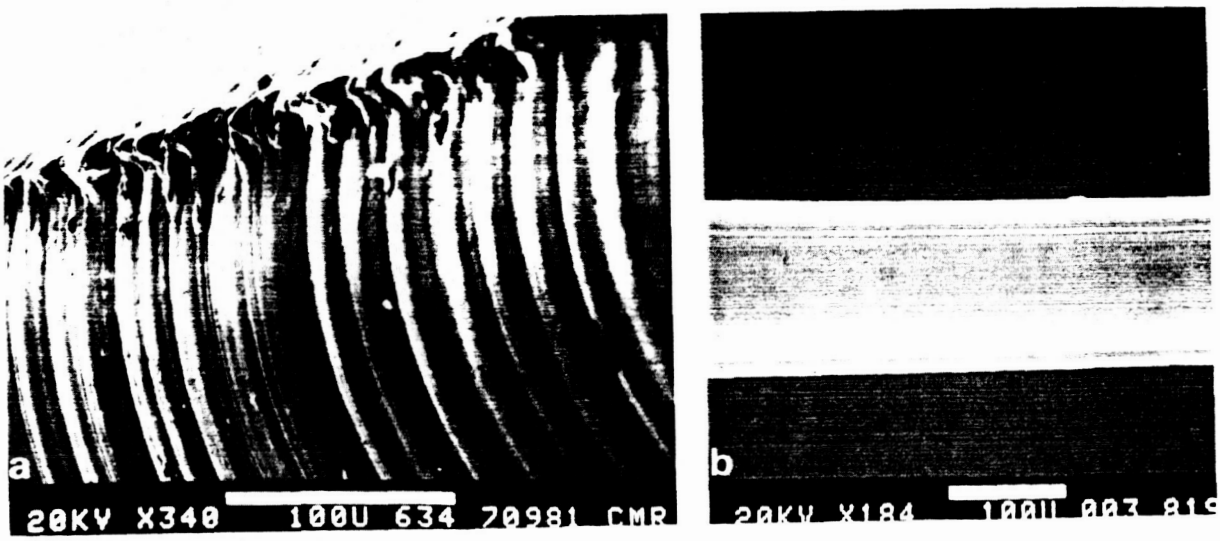

Fig. 4. Diameter variations in *c*-axis $LiNbO_3$ fibers: (a) large irregularities in diameter and rough growth ridges due to poor temperature and zone stability and (b) good diameter control and very uniform growth ridges.

The laser-heated pedestal growth (LHPG) method therefore, is one of the most versatile and perhaps simplest of crystal growth methods. With it, single crystal fibers of over 50 different materials have been grown to date, including oxides, halides, borides, carbides, metals, and semiconductors. A more detailed description of the history of fiber growth and the LHPG method can be found in refs. 1-3.

References

1. R. S. Feigelson, Growth of Fiber Crystals, in Crystal Growth of Electronic Materials, Ed. E. Kaldis (North-Holland, Amsterdam, 1985) p. 127.

2. R. S. Feigelson, W. L. Kway, and R. K. Route, Opt. Eng. 24 (1985) 1102.

3. R. S. Feigelson, J. Crystal Growth 79 (1986) 669-680.